In situ measurement of CO_2 and CH_4 from aircraft over northeast China and comparison with OCO-2 data

Xiaoyu Sun[1,2], Minzheng Duan[*1,2,3], Yang Gao[4], Rui Han[2,5], Denghui Ji[1,2], Wenxing Zhang[1], Nong Chen[6], Xiangao Xia[1,2], Hailei Liu[3], Yanfeng Huo[7]

[1]LAGEO, Institute of Atmospheric Physics, Chinese Academy of Sciences, 100029 Beijing, China
[2]College of Earth and Planetary Sciences, University of Chinese Academy of Sciences, Beijing,100049, China
[3]Chengdu University of Information Technology, Chengdu, 610225, China,
[4]China Meteorological Administration, Beijing, 100089, China
[5]ICCES, Institute of Atmospheric Physics, Chinese Academy of Sciences, Beijing, 100029, China
[6]Heilongjiang Meteorological Bureau, Harbin, 150001, China
[7]Anhui Meteorology Service, Hefei, 230061, China

Corresponding to: Minzheng Duan (dmz@mail.iap.ac.cn)

Abstract. Several satellites have been launched to monitor the increasing concentrations of greenhouse gases, especially CO_2 and CH_4 in the atmosphere, through back-scattered hyperspectral radiance in the shortwave infrared (SWIR) band. The vertical profiles of greenhouse gases and aerosol could strongly affect the results from these instruments. To investigate the effects of the vertical distribution of CO_2 on uncertainty in SWIR satellite retrieval results, we conducted observations of the vertical profiles of CO_2, CH_4, and aerosol particles at 0.6–7 km above sea level using a Beechcraft King Air 350ER in Jiansanjiang (46.77°N, 131.99°E), Heilongjiang province, Northeast China, on August 7–12, 2018. The profiles from this aircraft captured a decrease in CO_2 from 2 km to the minimum altitude due to uptake from vegetation at the surface in summer. CH_4 measurements showed an average 0.5 ppm increase from 2.0 to 0.6 km, which may result from emissions from the large area of paddy fields below, and a constant mole fraction between 1.951 and 1.976 ppm was recorded at 2 km and above. Comparison of CO_2 profiles from a new version of the carbon cycle data assimilation system Tan-Tracker (v1), retrievals from OCO-2 and aircraft measurements was conducted. The results from OCO-2 and the assimilation model system Tan-Tracker captured the vertical structure of CO_2 above 3 km, whereas below 3 km, the values from OCO-2 and Tan-Tracker model were lower than those from in situ measurements. Column-averaged CO_2 ~~volume mixing ratio~~volume mole fractions calculated from in situ measurements showed biases of _−4.68 ± 0.44_~~−2.39 ± 2.02~~ ppm and _−1.18% ± 0.11%_~~−0.61 ± 0.49%~~ compared to OCO-2 retrievals.

1 Introduction

Global warming due to greenhouse gases (GHGs) has become one of the most urgent and widely studied issues facing scientists in recent years. The Fifth Assessment Report of the Intergovernmental Panel on Climate Change (IPCC) noted that the global average temperature has increased by 0.85°C over the period 1880–2012. GHGs, especially the increasing CO_2 levels in the

atmosphere related to anthropogenic activity, are blamed for global warming, because they absorb and emit radiant energy within the thermal infrared range. Emission of CO_2 from fossil fuel combustion and industrial processes has contributed about 78% of the total GHG emissions increase from 1970 to 2010 (IPCC, 2015). Accurate measurement of CO_2 concentrations and

35   their spatial and temporal variations in the atmosphere is essential for estimation of sources and sinks in regional and global models. The Global Atmospheric Watch program (http://www.wmo.int/gaw) coordinates the systematic observation and analysis of GHGs and other trace substances, providing an important source of local and global GHG data. However, ground-based and in situ measurements near the surface can only provide information about the lower atmosphere, and are insufficient for analysis of total-column GHGs, which exhibits variations in both vertical and horizontal directions. Over the past few years,

40   several satellites, including the Greenhouse Gases Observing Satellite (GOSAT, launched in January 2009), Second Orbiting Carbon Observatory, (OCO-2, launched in 2014), and TanSat (launched in 2016), have been launched into space to monitor CO_2 by observing back-scattered hyperspectral radiance in shortwave infrared (SWIR) wavelength, which can provide ~~all-weather, all day~~ global coverage of the column-averaged dry-air mole fraction of CO_2 ~~volume mixing ratio~~ (X_{CO2}). Studies have shown that, given a 1–2 ppm accuracy of X_{CO2}, the use of space-borne instrument data can reduce the uncertainties in

45   regional ($8° \times 10°$ footprint) estimation of CO_2 sources and sinks (Rayner and O'Brien, 2001). In addition, CO_2 vertical profiles in the 5–25 km altitude range can be obtained using limb viewing space-borne sounders such as the Atmospheric Chemistry Experiment Fourier Transform Spectrometer (ACE-FTS, launched in August 2003). Foucher et al. (2009) reported the feasibility and difficulties of obtaining vertical CO_2 profiles using this method.

To validate and calibrate the X_{CO2} data from satellite measurement products, the Total Carbon Column Observing Network

50   (TCCON), a network of ground-based solar Fourier transform spectrometers operating in the SWIR spectral region was established (Wunch et al., 2011). Several studies have been conducted to determine X_{CO2}, the column-averaged CH_4 ~~volume mixing ratio~~ volume mole fraction (X_{CH4}), and the column-averaged ~~volume mixing ratio~~ volume mole fractions of other trace gases (X_{gas}) from TCCON data, which have shown good accuracy (Hedelius et al., 2017; Mendonca et al., 2019). In addition, commercial mobile solar-viewing near-infrared spectrometers of lower resolution than the TCCON instruments, such as

55   Bruker^{TM} EM27/SUN, show potential for measurement of X_{gas} with an acceptable bias range (Hedelius et al., 2016).

Retrieval accuracy is affected by knowledge of the vertical distribution of aerosols and CO_2. Vertical profiles of CO_2 also affect the accuracy of estimation for regional carbon fluxes in transport modeling, and can help elucidate the global carbon cycle and climate change. Many experiments have been conducted to measure the vertical profiles of CO_2, CH_4, and other trace gases. The AirCore sampling system can be used to obtain vertical profiles of CO_2 and CH_4 from near the surface to 8–

60   12 km with high accuracy (Karion et al., 2010; Membrive et al., 2017). Active remote sensing of atmospheric X_{CO2} with the Raman lidar (light detection and ranging) technique has been developed and used to measure CO_2 vertically in the troposphere (Zhao et al., 2007; Gong et al., 2013; Han et al., 2017). CO_2 concentrations were measured at 8–12 km by Tohoku University (Sendai, Japan) through flask sampling on a commercial airliner operated by Japan Airlines (JAL) between Japan and Australia in 1984 and 1985 (Nakazawa et al., 1991). The Comprehensive Observation Network for TRace gases by AIrLiner

65   (CONTRAIL) project installed continuous CO_2 measurement equipment onboard aircraft operated by JAL for in situ

measurement (Machida et al., 2008). The data for CONTRAIL are collected at altitudes between a few kilometers and 10 km, taking advantage of the frequent movement of commercial aircraft around the world. The Civil Aircraft for Remote Sensing and In Situ Measurements Based on the Instrumentation Container Concept (CARIBIC) project (Brenninkmeijer et al., 1999; Brenninkmeijer et al., 2007) aimed to observe trace gases such as CO, O_3, and CO_2 by deploying measurement equipment in passenger aircraft. The HIAPER Pole-to-Pole Observation (HIPPO) project involved a sequence of five global aircraft measurement programs to sample the atmosphere from near the North Pole to the coastal waters of Antarctica (Wofsy, 2011). Direct measurements that are independently collected from aircraft provide validation information for satellite products. Several studies have shown that profile measurements of CO_2 and CH_4 obtained using aircraft and AirCore are useful for bias correction of both TCCON measurements (Deutscher et al., 2010; Hedelius et al., 2016) and satellite products (Araki et al., 2010; Inoue et al., 2013, 2014; Miyamoto et al., 2013; Frankenberg et al., 2016; Wunch et al., 2017).

Three satellites designed for CO_2 measurement, TanSAT (Yang et al., 2018; Yang et al., 2020), GMI/GF-5 (Li et al., 2016), and GAS/FY-3D (Qi et al., 2020), were launched into space in 2016, 2017, and 2018, respectively. Measurement of profiles is crucial to further validate the retrieved hyperspectral measurements from these three satellites. Because the algorithm for satellite retrieval requires a prior profiles based on the model and in situ measurements, the lack of direct and independent airborne observations may increase the bias in the satellite results over China.

In this study, in situ aircraft-based measurements of CO_2 and CH_4 were conducted in Jiansanjiang, Northeast China, in August 2018. An ultraportable greenhouse gas analyzer (UGGA; model 915-0011; Los Gatos Research, San Jose, CA, USA) was used onboard the aircraft to measure the vertical mole fractions of CO_2 and CH_4 at altitudes of 0.6–7 km. Descriptions of the aircraft and onboard instruments are provided in Section 2. Details of the experimental site and the flight trajectory are provided in Section 3. A comparison of the profiles obtained using aircraft with OCO-2 and the assimilation system Tan-Tracker (v1) is described in Section 4. Finally, the methods used to calculate X_{CO2} and extrapolate in situ profiles, as well as error estimation, are discussed in Section 5.

2 Methods~~Instruments~~

2.1 Aircraft Instrumentation

The aircraft used for this experiment was a Beechcraft King Air 350ER, which is a twin-turboprop aircraft designed for weather modification missions and measurement of trace gases and aerosols by the China Meteorological Administration (CMA). The cruising speed and maximum speed of the aircraft are 441 and 561 km/h, respectively. ~~Geolocation data for the aircraft, such as Global Positioning System height, latitude, and longitude, were recorded with the corresponding local time during each flight.~~ Temperature, wind speed, relative humidity, and other meteorological data were detected and recorded by an Aircraft Integrated Meteorological Measurement System (~~AIMMS~~AIMMS-20AG) installed on the aircraft. The geolocation information including latitude, longitude, ambient pressure and height of the aircraft is also measured by AIMMS-20AG. The

3

relative humidity is calculated by temperature and dew point, measured by the Total Temperature Sensor (Model 102 Type Non-De-iced, Rosemount Aerospace Inc) Dew Point Hygrometer (Model 137 Vigilant™, EdgeTech), respectively.

The ultraportable greenhouse gas analyzer, UGGA (model 915-0011; Los Gatos Research), was connected to an aircraft-based impactor inlet system which consists of CVI (Model 1204; Brechtel Manufacturing Inc.) and ISO inlet (Model 1200; Brechtel Manufacturing Inc.)(CVI Model 1204; Brechtel Manufacturing Inc., Hayward, CA, USA) in the pressurized cabin for continuous measurement of CO_2 and CH_4. The CVI inlet, mounted on top of the aircraft body, maintained an air sample flow rate of 15 L/min using a mass flow controller. The CVI and/or ISO inlet was mounted on the top of the aircraft body as shown in figure 1, and the air flow rate of the inlet is kept constant by the automatic air flow controller of the inlet (Aircraft-based Counterflow Virtual Impactor Inlet System CVI - Model 1204, Brochure; Isokinetic Inlet System ISO Inlet - Model 1200, Brochure). The UGGA uses a laser absorption technology called off-axis integrated cavity output spectroscopy to determine the trace gas concentration with a high precision of < 300 ppb (CO_2) and < 2 ppb (CH_4) and a 10-s response time (UGGA user manual, model 915-0011; Los Gatos Research) and was tested and controlled in the laboratory. As shown in the in-flight schematic diagram (figure 1), the external oil-less diaphragm vacuum pump (F-9A 08-03, GAST) was mounted between the CVI inlet and/or the ISO inlet, with the maximum pressure of 31.15 lpm (litter per minute) used to keep a stable airflow. The ISO inlet was used as the aircraft pass through clouds, and CVI inlet was used in the other times. Similar system for airborne GHG measurement have been reported by O'Shea et al. (2013) and Palmer et al. (2013).

The absolute pressure of the cell was kept constant (66.67 hPa) by an automatic pressure controller, and the absolute temperature was kept within the range of 26.80–33.05°C. During the flight, the pressure of the sample cavity was kept constant by an small pump inside the instrument with the airflow about 0.3 lpm. The sample cavity temperature was also kept stable and constant by the temperature controller of the instrument. The instrument automatically recorded and saved the temperature and pressure in the cavity during operation. According to the records, the standard deviation of the cell pressure during three flights is 0.029, 0.029, 0.033 on 7, 9 and 10 August and the range of the cell pressure on each flight is below 0.12 torr. For the cell temperature, the standard deviation is 0.46, 1.55 and 1.18 on each day and the range is below 3.11℃. The UGGA was calibrated against standard GHGs (provided by the National Institute of Metrology, China) before takeoff and after landing of each flight to ensure the accuracy of the data measured with the UGGA. Before this study, the GHG standard gases have been used by the CMA, Chinese Academy of Sciences, and other scientific research institutions for calibration and validation, showing that these standard gases have good performance and reliability. The standard gas we used is based on dry and clean air with greenhouse gases known concentration value, filled in a 29.5L aluminum alloy cylinder with silanization and other special treatment on the inner wall, traceable to the world meteorological organization global atmospheric observation network (WMO-GAW) level 1 standard gas. The concentration of the CO_2 is 400.13 ppm and CH_4 is 1.867 ppm. The standard gas we use has been measured in the laboratory for the proportion of δ13C in CO_2. The range of the proportion is -8.0‰ to -8.2‰ close to the natural content, so it will not cause significant isotopic effect on the measurement of CO_2 by optical method and meet the requirements of standard gas (Yao et al., 2013). Just before taking off, UGGA was calibrated against standard gas, and the stability of instrument was checked and tested again using the same standard gas of CO_2 and CH_4 immediately after

4

landing. As shown in Figure 2, the concentration of CO_2 and CH_4 before and after landing is stable around the value of standard has concentration, and there is almost no drift after the flight. The precision and reparability of the instruments are also checked and test multiple times in laboratory and the results show that it is stable and good for the measurements.

2.2 Tan-Tracker and OCO-2 data

135 Based on the nonlinear least squares four-dimensional variational data assimilation algorithm (NLS-4DVar) and the Goddard Earth Observing System atmospheric chemistry transport model (GEOS-Chem), Tan-Tracker provides surface flux inversion estimates and profiles of CO_2 with 47 levels of vertical resolution from the surface to 0.03 hPa and horizontal resolution of $2.5° \times 2°$. The NLS-4DVar assimilation model Tan-Tracker (v1) and OCO-2 X_{CO2} (v9r) retrievals are used to optimize surface terrestrial ecosystem CO_2 flux and ocean CO_2 flux, while prior Fossil Fuel emission and prior Fire emission remain unchanged

140 (details of model setting and prior flux information can be found in Han and Tian, 2019).

The Orbiting Carbon Observatory-2 (OCO-2), successfully launched on 2 July 2014, obtained global measurement of CO2 through hyperspectral measurement of reflected sun light from earth atmosphere in one NIR and two SWIR bands centre at 0.76, 1.61 and 2.06 µm, more details about the mission, retrieving algorithm and data characteristic can be found in– Crisp et al. (2008) and O'Dell et al. (2012). The uncertainty and bias of the X_{CO2} products related to surface properties, aerosol and

145 cloud, and the retrieving algorithm has been reported by Butz et al. (2009), Jung et al. (2016) and Connor et al. (2016). The OCO-2 data (V9r) including X_{CO2}, CO_2 profile and the a priori profile was used in this study.

3 Experimental Site

~~Aircraft measurement was carried out from August 7 to 10 over Jiansanjiang (47.11°N, 132.66°E, 61 m above sea level), which is located in Heilongjiang province, Northeast China (solid circle, Figure 1).~~ Aircraft measurement were carried out from 7 to

150 10 August over Jiansanjiang (47.11°N, 132.66°E, 61 m above sea level), located in Heilongjiang province, Northeast China. Figure 3 shows the geolocation of the Jiansanjiang aircraft and the fight path. The area is mostly covered with large tracts of farmland. Rice cultivation is carried out primarily in summer, and crop growth is vigorous during this period. Due to the influence of plant photosynthesis, a large amount of CO_2 uptake occurs near the surface.

Three profiles were obtained between around 08:00 and 11:00 in local time (GMT+8) on 7, 9 and 10 August, 2018. ~~Three~~

155 ~~profiles were obtained between 08:00 and 11:00 on August 7, 9, and 10.~~ The aircraft is designed for weather modification by China Meteorological Administration (CMA), so the infrastructure of the aircraft and the gas flow system are also designed and completed in USA by the team of weather modification agency and an US company. CMA is in charge of the flight route, and there is a chance (several times later are planning) that it can carry the greenhouse gas analyzer to measure the profiles of CO_2 and CH_4. The greenhouse gas analyzer was loaded on the aircraft and some parts of air flow arrangements were modified

160 to better fit the requirement for greenhouse profile measurement. Due to the logistical problem and the ATC restriction, we

must fly in the morning from around 7:30 to 11:00 (local time) of these days to avoid obstructing civil aviation. The details of the three flights are listed in table 1.

Figure 2 shows the flight path followed on August 7, when the flight climbed quickly to about 7.5 km after takeoff and then spiraled down toward the surface slowly, over a horizontal distance of about 150 km.

165 The flight trajectory on 7 August is shown in figure 4. The aircraft climbed up quickly and directly to the maximum height to about 7.5 km 30 min after taking off, and then descending down step by step at about every 300 m. Since the 3-D figure in these three days looks identical, the flight trajectory of the other two days (9 and 10 August) is not shown in figure 4. Considering the sensitivity of the UGGA response, measurements collected during the ascent were discarded due rapid changes in air pressure, and only data collected and reserved while spiraling downward were regarded as valid and analyzed further.

170 Data recorded below 0.6 km were also rejected because samples were easily contaminated with exhaust emissions during the slowing and descent of the aircraft before landing. The spiral descent of the aircraft lasted for about 2.5 h on each of the three sampling days.

4 Data Processing

4.1 Water vapor correction

175 The mixing ratiomole fraction of CO_2 or CH_4 measured during flight is the volume in proportion to air containing water vapor, which cannot be directly compared with values from other data sources due to differing water vapor contents of the sampled air. Therefore, the effect of water vapor is corrected and mixing ratiomole fractions of CO_2 and CH_4 to dry air are given by:

$$f_{gas\_dry} = \frac{f_{gas} \cdot p}{p - p_{H_2O}}$$
(1)

where f_{gas_dry} (mol/mol) is the mole fraction of a gas in dry air, and f_{gas} (mol/mol) is the measured mole fraction of gas under real air conditions with water vapor. P_{H_2O} is water vapor pressure in hPa, which can be calculated as:

$$p_{H_2O} = e_s \cdot RH$$
(2)

180 where e_s (hPa) is the saturated water vapor pressure at temperature T (K) at aircraft altitudes, which can be derived from the Clausius–Clapeyron equation:

$$\ln \frac{e_s}{6.11} = \frac{L_v M_w}{R}(\frac{1}{273} - \frac{1}{T}) \approx 5.42 \times 10^3 (\frac{1}{273} - \frac{1}{T}).$$
(3)

where L_v is the latent heat of vaporization, M_w is the molecular weight of water, and R is the gas constant. Temperature T (K), relative humidity RH (%), and pressure p (hPa) of the ambient atmosphere are measured using the aircraft meteorology system, AIMMS. Where $L_v = 2.500 \times 10^6$ J Kg^{-1}, M_w is the molecular weight of water equals to 18.016, R = 8.3145 J $K^{-1}mol^{-1}$, and e_s

185 (in hPa) at temperature T (in K). Pressure p (hPa) of the ambient atmosphere are measured by the aircraft meteorology system, AIMMS-20AG, and the temperature T (K) was measured by Total Temperature Sensor (Model 102 Type Non-De-iced). The

relative humidity RH (%) was calculated by the dew point and temperature. The dew point data is obtained by Dew Point Hygrometer (Model 137 Vigilant™, EdgeTech).

4.2 Data processinginterpolation

Before aircraft takeoff, the clocks of both the UGGA, and AIMMS-20AG, the Total Temperature Sensor and other instruments were adjusted to match those of the CO_2, CH_4, and weather system measurements, synchronizing these data to the altitude and geolocation of the aircraft. The data from UGGA and synchronous meteorology measurements, including temperature, pressure, and humidity of ambient atmosphere, are recorded every second, then smoothed with a 10-s running average to further remove errors caused by temporal mismatch considering the response time of the UGGA. Because the flights followed a spiral trajectory that descended approximately every 300 m, only data collected during level flight were retained and analyzed, whereas data from the descent periods were removed to avoid effects from vertical variations in sampling during rapid descent. The time points at the beginning and end of level flight are determined according to the altitude and its variation of the aircraft. Considering the residual time of the GHG measurement system, the data obtained 220s from the start of the level flight is considered to be observed when the aircraft is descending rather than in level, which may cause uncertainty of the measurement. Therefore, the data were reserved after the level flight starting for 220s. If the duration time of certain level flight lasted less than 220s, the data observed during that level flight were also discarded.

The instrument was calibrated against the standard gas before and after each flight. All of the measurements during the calibration process, including the standard gas used for calibration can trace back to WMO scale. The maximum and the average value of the difference between the standard gas and the measurement of the instrument of each day was considered as the accuracy of the aircraft data. For the precision, noted that the instrument was not continuously calibrated against the standard gas during the flight, we calculated the one standard deviation of the data in each level flight, and the maximum of the average value of 1-σ on each day is considered as the precision of the aircraft measurement. The accuracy of CO_2 and CH_4 is below 0.66 ppm and 0.002 ppm, 0.16% and 0.10% of the CO_2 and CH_4 concentration in standard gas, respectively. For precision, the 1-σ value is below 0.71 ppm and 0.0062 ppm for CO_2 and CH_4, respectively.

5 Results and Discussion

5.1 CO_2 and CH_4 profiles

Figure 53 shows vertical profiles of the CO_2 and CH_4 mole fractions measured with the UGGA during the flight campaign over Jiansanjiang, which is an agricultural area that produces a large amount of rice. The CO_2 concentration increased with height in the troposphere (Figure 53a), which may have resulted from CO_2 uptake by rice plants near the surface during the summer growth season. The greater increase rate of CO_2 in the lower troposphere on August 77 August compared to the other two days was probably attributed to differing weather conditions on the three sampling days. August 77 August was a sunny

day, but it was overcast on ~~August~~ 9 and 10, August, which may have weakened photosynthesis in rice and reduced CO_2 uptake. During all three flights, the mole fraction of CO_2 reached a maximum of about 418 ppm in the free troposphere at the top of the profile.

The ~~mixing ratio~~mole fraction of CH_4 showed a consistent decrease in concentration with height, ranging from 1.95 to 2.10 ppm from about 2 km to near the surface, which may have been the result of CH_4 emissions from agricultural activity at the surface. CH_4 showed low variability of less than 0.5 ppm at higher altitudes, from above 2 to 7 km, indicating a well-mixed vertical structure of CH_4 in the free troposphere.

Comparing the CO_2 and CH_4 observation data, the mole fraction of CH_4 varied less than that of CO_2 from 1.5–2 km up to the free troposphere, with a stable value of about 1.925 ppm. This stability indicated that CH_4 was evenly mixed at these heights and that there were no obvious sources or sinks of CH_4. Conversely, CO_2 rose with increasing altitude in the free troposphere from about 400 to 418 ppm. This increase may have been due to photosynthesis by vegetation and the large number of crops planted locally, creating a CO_2 sink at the surface, and causing the CO_2 concentration to rise with height in the free troposphere. Our findings indicate that the vertical profile of CO_2 in summer increases with height in the upper troposphere, whereas that of CH_4 changes little with height and is relatively stable.

5.2 Comparison of profiles from the model and satellite product

Aircraft measurements were compared with CO_2 data obtained from OCO-2 (v9r) retrievals and the recently developed data assimilation system for the global carbon cycle, Tan-Tracker (v1) (Han and Tian, 2019). ~~Based on the nonlinear least squares four-dimensional variational data assimilation algorithm (NLS-4DVar) and the Goddard Earth Observing System atmospheric chemistry transport model (GEOS-Chem), Tan-Tracker provides accurate surface flux inversion estimates and profiles of CO_2 with 47 levels of vertical resolution from the surface to 0.03 hPa and horizontal resolution of 2.5° × 2°.~~ The assimilation data are collected and linearly interpolated spatially and temporally based on the geolocation of the observation site and time. Because no data were obtained from OCO-2 (v9r) over Jiansanjiang during the flight, the results of OCO-2 within 1° × 1° spatially at the closest time to the flight, which were collected on 5 August were used for comparison. The height of the profile is available on the satellite product.

The structure~~variation~~ of CO_2 varied with height could be roughly divided into three segments: surface to 2 km, 2 to 3 km, and 3 to 8 km (Figure 6~~4~~). Below 2 km, CO_2 of Tan-tracker model is assumed to be well mixed and uniformly distributed with height, with values ranging from 385 to 395 ppm; therefore, the model could not reproduce the strong decrease in CO_2 from 2 km to the surface due to uptake by vegetation. From 2 to 3 km, CO_2 increased to about 400 ppm with altitude. The averaged satellite retrieval profiles correctly reproduced the decrease in CO_2 from 2 km to the surface, but the decrease rate was lower than those of in situ profiles, decreasing from 393 ppm at 2 km to 390 ppm near the surface. Flight data showed a significant CO_2 sink in this region, most notably on ~~August~~ 7 August, when it decreased from 400 ppm at 2 km to 380 ppm at 0.6 km. The impact of ground sinks was more pronounced and apparent than in results from satellite inversion and model simulations, indicating that the strong variations in the lower atmosphere and planetary boundary layer (PBL) should be more carefully

8

250 considered in model~~ing~~ and retrieval algorithms. Between 2 and 4 km, aircraft profiles showed a relatively uniform mixing level of CO_2, with roughly stable concentrations around 400 ppm.

In general, all profiles from aircraft, satellite retrieval, and model~~ing~~ showed a similar vertical distribution trend in the troposphere above 2 km, but with large differences in values. The ~~volume mixing ratio~~volume mole fraction ~~s~~ of CO_2 from both satellite and aircraft measurements indicated a CO_2 sink. GHGs profiles have been rarely observed before near the

255 experiment site, or over Northeast of China as far as we know. The model simulations are based on data of regional emission inventory. The accuracy of simulated profiles and concentration near surface over the experiment site still remains unknown. So continuous and regular observation of the GHGs profiles are necessary to better understand the regional emission amounts and the variation of the GHGs.

260 **5.3 Comparison of X_{CO2} products**

The total column amount of CO_2, can be derived by integrating the CO_2 concentration from the surface to the top of the atmosphere under the assumption of hydrostatic conditions:

$$VC_{CO_2} = \int_0^{P_s} \frac{f_{CO_2}^{dry} \cdot (1 - f_{H_2O})}{g(p) \cdot m(p)} dp$$
$$m = [m_{H_2O} \cdot f_{H_2O} + m_{air}^{dry} \cdot (1 - f_{H_2O})]$$

(4)

where VC_{CO_2} is the total column amount of CO_2, $f_{CO_2}^{dry}$ is the dry-air mole fraction (DMF) of CO_2 (mol mol^{-1}), $f_{H_2O}(p)$ is the aircraft profile of H_2O (mol mol^{-1}), which is measured using the onboard AIMMS system, $m(p)$ is the mean molecular mass of

265 wet air, and $g(p)$ is gravitational acceleration, $m_{H_2O} = 18.02 \times 10^{-3}/N_A$ kg/molecule, $m_{air}^{dry} = 28.964 \times 10^{-3}/N_A$ kg/molecule, and N_A is Avogadro's constant. Data beyond the flight limit are taken from National Centers for Environmental Prediction (NCEP) reanalysis data interpolated to the time of flight.

The column-averaged DMF of CO_2 (X_{CO2}) from aircraft measurements was calculated based on the method of Wunch et al. (2010), which considers the average kernel in OCO-2 satellite retrievals:

$$X_{CO_2}^{in\ situ} = X_{CO_2}^{a} + \sum_j h_j a_j (t_{in\ situ} - t_a)_j$$

(5)

270 where a is the average kernel (Rodgers and Connor, 2003), $X_{CO_2}^{a}$ is the column-averaged DMF for the a priori profile t_a, h_j is the pressure weighting function of OCO-2, and $t_{in\ situ}$ is the in situ profile from aircraft measurement.

Because in situ measurements available from aircraft are limited, values outside of the aircraft's vertical observation range must be estimated to calculate X_{CO2}. Two extrapolation methods were used to extend the profile of the aircraft measurements and then estimates the X_{CO2} value of the in-situ measurement respectively. 1) The unknown part of the aircraft profile was

275 directly from the OCO-2 a prior profile. 2) A well-mixed and constant mixing ratio of CO_2 is assumed from the surface to the

lower limit of flight, and from the upper limit of flight to the tropopause. The CO_2 concentrations above the tropopause were calculated with an empirical model (Toon and Wunch, 2014) which considers tropopause height as well as realistic latitude and time dependencies through curve fitting of data from high-altitude balloons, AirCore, Observations of the Middle Stratosphere balloon, and aircraft. In general, the mole fraction of CO_2 decreased exponentially with height from the tropopause

280 to upper stratosphere, and the tropopause height was obtained from NCEP reanalysis data with a 2.5° × 2.5° resolution, which was linearly interpolated to the geographic coordinates of Jiansanjiang. Figure 7 shows the extrapolated CO_2 profiles using method (2)A well-mixed and constant mixing ratio of CO_2 is assumed from the surface to the lower limit of flight, and from the upper limit of flight to the tropopause. The CO_2 concentrations for the stratosphere and above were calculated with an empirical model (Toon and Wunch, 2014) that considers tropopause height as well as realistic latitude and time dependencies

285 through curve fitting of data from methods such as high-altitude balloons, AirCore, Observations of the Middle Stratosphere balloon, and aircraft. In general, the mole fraction of CO_2 decreased exponentially with height from the tropopause to upper stratosphere, and the tropopause height was obtained from NCEP reanalysis data with a 2.5° × 2.5° resolution, which was linearly interpolated to the geographic coordinates of Jiansanjiang..

X_{CO2} calculated from aircraft measurements and differences with that from OCO-2 are listed in Table 1 and 2. Because no data

290 were obtained from OCO-2 over Jiansanjiang during the flight, the results of OCO-2 within 1° × 1° spatially at the closest time to the flight, which were collected on August 5, were used for comparison. The results showed that X_{CO2} values from OCO-2 were lower, with an average difference of −4.68−2.39 ± 0.442.02 ppm (−1.180.59% ± 0.440.11%) and -5.09 ± 1.28 ppm (-1.28% ± 0.32%) by method (1) and by method (2).

295 Uncertainties induced by extrapolation of profiles outside the height limits of aircraft flight and by errors in tropopause estimation were analyzed. Errors in extrapolation of the profile below the lower limit and above the upper limit of flight were estimated by recalculating X_{CO2} after a 1-ppm positive shift in the CO_2 concentrations at these altitudes. For method (1), since the value of CO_2 mole faction of unknown part is the same as that of the OCO-2 a priori profile, as eq. (5) shows, no extra uncertainty would be introduced by extrapolation. But for method (2), As the profile is assumed to decrease exponentially with

300 height above the tropopause, the height of the tropopause also introduces uncertainties for X_{CO2}. Table 2 lists the errors resulting from three sources: 1) uncertainties from in situ measurement, 2) extrapolation of the profile in the PBL where no in situ measurements were collected, and 3) profile assumptions above the upper limit of flight observations. Errors due to uncertainty in tropopause height were analyzed by shifting the tropopause height upward by 1 km, and the results are also listed in Table 2. These results indicated that the extrapolation method and assumptions used to construct profiles where no measurements

305 were made were the primary source of errors, among which the greatest error was from the profile above the upper limit of the flight (0.323.34 ppm, 0.85%). Errors due to uncertainty in the tropopause height were also non-negligible. Because of the lack of observation data near the surface, the missing measurement data was directly replaced by the data at the lowest altitude measured by the aircraft. The error caused by this practice is shown in table 3, with an average of 0.79 ppm for X_{CO2}. This is also the impact of the lack of near-surface observations on the overall X_{CO2} estimates. Therefore, observations from near the

10

310 surface to about 1 km from other method, such as in-situ GHG measurement by tethered balloon and high tower, is necessary for accurate estimation of X_{CO_2}.

6 Conclusion

The vertical distributions of CO_2 and CH_4 were measured using a Beechcraft King Air 350ER over Jiansanjiang, an extensive

315 paddy area in Northeast China, and three vertical profiles from 0.6 to 7.5 km were obtained on ~~August 7, 9, and 10~~7, 9 and 10 August. Measurements of the mole fraction of CO_2 showed an increase with height, whereas CH_4 decreased with height. These results are reasonable, because paddies are a sink for CO_2 and source of CH_4 during the summer growing season. Comparing the observed profiles from aircraft with those from the carbon cycle data assimilation system Tan-Tracker (v1) and OCO-2 retrievals showed that the general vertical structure was consistent, but the values of mole fraction of CO_2 from Tan-Tracker

320 and OCO-2 had negative bias estimates. The average bias between aircraft and OCO-2 is -4.68 ± 0.44 ppm ($-1.18\% \pm 0.11\%$)~~but the values of mole fraction of CO_2 from Tan-Tracker and OCO-2 had negative bias estimates of -2.39 ± 2.02 ppm and $0.59 \pm 0.44\%$, respectively~~. The uncertainty arose mainly from extrapolation of the profile beyond the flight limit, where no in situ measurements were available.

Data availability

325 Data used in this study are available from the corresponding author upon request (dmz@mail.iap.ac.cn).

Author contributions

M. Duan and X. Sun determined the main goal of this study. X. Sun carried it out, analyzed the data, and prepared the paper with contributions from all co-authors. Y. Gao and N. Chen provided technical guidance for related instrument.

Competing interests

330 The authors declare that they have no conflict of interest.

Acknowledgements

experiment and the instrumentation onboard the aircraft. We also thank Jiansanjiang Airport for providing the experimental
335 site and arranging time for conducting the campaign.

References

Araki, M., Morino, I., Machida, T., Sawa, Y., Matsueda, H., Ohyama, H., Yokota, T., and Uchino, O.: CO 2 column-averaged
  volume mixing ratio derived over Tsukuba from measurements by commercial airlines, Atmos. Chem. Phys., http://doi:10,
  7659-7667, 2010.

340 Brenninkmeijer, C., Crutzen, P., Boumard, F., Dauer, T., Dix, B., Ebinghaus, R., Filippi, D., Fischer, H., Franke, H., and Frieβ,
  U.: Civil Aircraft for the regular investigation of the atmosphere based on an instrumented container: The new CARIBIC
  system, Atmos. Chem. Phys., 7, 4953-4976, https://doi.org/10.5194/acp-7-4953-2007, 2007.

Brenninkmeijer, C., Crutzen, P., Fischer, H., Güsten, H., Hans, W., Heinrich, G., Heintzenberg, J., Hermann, M., Immelmann,
  T., and Kersting, D.: CARIBIC—Civil aircraft for global measurement of trace gases and aerosols in the tropopause region,
345 J. Atmos. Ocean Technol., 16, 1373-1383, http://doi:10.1175/1520-0426(1999)016<1373:CCAFGM>2.0.CO;2, 1999.

Crisp, D., Miller, C. E., and DeCola, P. L.: NASA Orbiting Carbon Observatory: measuring the column averaged carbon
  dioxide mole fraction from space, J. Appl. Remote. Sens., 2, 023508, http://doi:10.1117/1.2898457, 2008.

Deutscher, N., Griffith, D., Bryant, G., Wennberg, P., Toon, G., Washenfelder, R., Keppel-Aleks, G., Wunch, D., Yavin, Y.,
  and Allen, N.: Total column CO2 measurements at Darwin, Australia-site description and calibration against in situ aircraft
350 profiles, Atmos. Meas. Tech., 2010. 2010.

Deutscher, N., Griffith, D., Bryant, G., Wennberg, P., Toon, G., Washenfelder, R., Keppel-Aleks, G., Wunch, D., Yavin, Y.,
  Allen, N., Blavier, J.-F., Jiménez, R., Daube, B. C., Bright, A. V., Matross, D. M., Wofsy, S. C., and Park, S.: Total column
  CO2 measurements at Darwin, Australia-site description and calibration against in situ aircraft profiles, Atmos. Meas.
  Tech., 3, 947-958, http://doi:10.5194/amt-3-947-2010, 2010.

355 Endresen, Ø., Sørgård, E., Behrens, H. L., Brett, P. O., and Isaksen, I. S.: A historical reconstruction of ships' fuel consumption
  and emissions, J. Geophys. Res. Atmos., 112, http://doi:10.1029/2006JD007630, 2007.

Foucher, P., Chédin, A., Dufour, G., Capelle, V., Boone, C., and Bernath, P.: Feasibility of CO 2 profile retrieval from limb
  viewing solar occultation made by the ACE-FTS instrument, Atmos. Chem. Phys., 9, 2873-2890, http://doi:10.5194/acp-
  9-2873-2009, 2009.

360 Frankenberg, C., Kulawik, S. S., Wofsy, S. C., Chevallier, F., Daube, B., Kort, E. A., O'dell, C., Olsen, E. T., and Osterman,
  G.: Using airborne HIAPER Pole-to-Pole Observations (HIPPO) to evaluate model and remote sensing estimates of
  atmospheric carbon dioxide, Atmos. Chem. Phys., 16, 7867-7878, http://doi:10.5194/acp-16-7867-2016, 2016.

Gong, W., Han, G., Ma, X., and Lin, H.: Multi-points scanning method for wavelength locking in CO2 differential absorption
  lidar, Opt. Commun., 305, 180-184, http://doi:10.1016/j.optcom.2013.05.006, 2013.

365 Han, G., Ma, X., Liang, A., Zhang, T., Zhao, Y., Zhang, M., and Gong, W.: Performance evaluation for China's planned CO_2-IPDA, Remote Sens., 9, 768, http://doi:10.3390/rs9080768, 2017.

Han, R. and Tian, X.: A dual-pass carbon cycle data assimilation system to estimate surface CO_2 fluxes and 3D atmospheric CO_2 concentrations from spaceborne measurements of atmospheric CO_2, Geosci. Model Dev. Discuss., https://doi.org/10.5194/gmd-2019-54, in review, 2019.

370 Hedelius, J. K., Parker, H., Wunch, D., Roehl, C. M., Viatte, C., Newman, S., Toon, G. C., Podolske, J. R., Hillyard, P. W., Iraci, L. T., Dubey, M. K., and Wennberg, P. O.: Intercomparability of $X_{\_}(CO_{\_}2)$ and $X_{\_}(CH_{\_}4)$ from the United States TCCON sites, Atmos. Meas. Tech., 10, 1481-1493, http://doi:10.5194/amt-10-1481-2017, 2017.

Hedelius, J. K., Viatte, C., Wunch, D., Roehl, C. M., Toon, G. C., Chen, J., Jones, T., Wofsy, S. C., Franklin, J. E., Parker, H., Dubey, M. K., and Wennberg, P. O.: Assessment of errors and biases in retrievals of X CO 2, X CH 4, X CO, and X N 2

375 O from a 0.5 cm–1 resolution solar-viewing spectrometer, Atmos. Meas. Tech., 9, 3527-3546, http://doi:10.5194/amt-9-3527-2016, 2016.

Inoue, M., Morino, I., Uchino, O., Miyamoto, Y., Saeki, T., Yoshida, Y., Yokota, T., Sweeney, C., Tans, P. P., Biraud, S. C., Machida, T., Pittman, J. V., Kort, E. A., Tanaka, T., Kawakami, S., Sawa, Y., Tsuboi, K., and Matsueda, H.: Validation of XCH 4 derived from SWIR spectra of GOSAT TANSO-FTS with aircraft measurement data, Atmos. Meas. Tech., 7, 2987-

380 3005, http://doi:10.5194/amt-7-2987-2014, 2014.

Inoue, M., Morino, I., Uchino, O., Miyamoto, Y., Yoshida, Y., Yokota, T., Machida, T., Sawa, Y., Matsueda, H., Sweeney, C. C., Tans P. P., Andrews A. E., Biraud S. C., Tanaka T., Kawakami S., and Patra, P. K.: Validation of XCO 2 derived from SWIR spectra of GOSAT TANSO-FTS with aircraft measurement data, Atmos. Chem. Phys., 13, 9771-9788, http://doi:10.5194/acp-13-9771-2013, 2013.

385 Jung, Y., Kim, J., Kim, W., Boesch, H., Lee, H., Cho, C., and Goo, T.-Y.: Impact of aerosol property on the accuracy of a CO_2 retrieval algorithm from satellite remote sensing, Remote Sens., 8, 322, http://doi:10.3390/rs8040322, 2016.

Karion, A., Sweeney, C., Tans, P., and Newberger, T.: AirCore: An innovative atmospheric sampling system, J. Atmos. Ocean Technol., 27, 1839-1853, http://doi:10.1175/2010JTECHA1448.1, 2010.

Keller, C. A., Long, M. S., Yantosca, R. M., Da Silva, A., Pawson, S., and Jacob, D. J.: HEMCO v1. 0: a versatile, ESMF-

390 compliant component for calculating emissions in atmospheric models, Geosci. Model Dev., 7, http://doi:10.5194/gmd-7-1409-2014, 2014.

Li, Y., Zhang, C., Liu, D., Chen, J., Rong, P., Zhang, X., and Wang, S.: CO_2 retrieval model and analysis in short-wave infrared spectrum, Optik., 127, 4422-4425, http://doi:10.1016/j.ijleo.2016.01.144, 2016.

Machida, T., Matsueda, H., Sawa, Y., Nakagawa, Y., Hirotani, K., Kondo, N., Goto, K., Nakazawa, T., Ishikawa, K., and

395 Ogawa, T.: Worldwide measurements of atmospheric CO_2 and other trace gas species using commercial airlines, J. Atmos. Ocean Technol., 25, 1744-1754, http://doi:10.1175/2008JTECHA1082.1, 2008.

Membrive, O., Crevoisier, C., Sweeney, C., Danis, F., Hertzog, A., Engel, A., Bönisch, H., and Picon, L.: AirCore-HR: a high-resolution column sampling to enhance the vertical description of CH4 and CO2, Atmos. Meas. Tech., doi: amt-10-2163-2017, 2017. http://doi:amt-10-2163-2017, 2017.

400   Mendonca, J., Strong, K., Wunch, D., Toon, G. C., Long, D. A., Hodges, J. T., Sironneau, V. T., and Franklin, J. E.: Using a speed-dependent Voigt line shape to retrieve O 2 from Total Carbon Column Observing Network solar spectra to improve measurements of XCO 2, Atmos. Meas. Tech., 12, 35-50, http://doi:10.5194/amt-12-35-2019, 2019.

Miyamoto, Y., Inoue, M., Morino, I., Uchino, O., Yokota, T., Machida, T., Sawa, Y., Matsueda, H., Sweeney, C., Tans, P., Andrews, A. E., and Patra, P. K.: Atmospheric column-averaged mole fractions of carbon dioxide at 53 aircraft

405   measurement sites, Atmospheric Chemistry & Physics Discussions, 12, http://doi:10.5194/acp-13-5265-2013, 2012.

Miyamoto, Y., Inoue, M., Morino, I., Uchino, O., Yokota, T., Machida, T., Sawa, Y., Matsueda, H., Sweeney, C., Tans, P. P., Andrews, A. E., Biraud, S. C., and Patra, P. K.: Corrigendum to "Atmospheric column-averaged mole fractions of carbon dioxide at 53 aircraft measurement sites" published in Atmos. Chem. Phys. 13, 5265–5275, 2013, Atmos. Chem. Phys., 13, 9213–9216, https://doi.org/10.5194/acp-13-9213-2013, 2013.

410   Nakazawa, T., Miyashita, K., Aoki, S., and Tanaka, M.: Temporal and spatial variations of upper tropospheric and lower stratospheric carbon dioxide, Tellus., 43, 106-117, http://doi:10.1034/j.1600-0889.1991.t01-1-00005.x, 1991.

O'Brien, D. and Rayner, P.: Global observations of the carbon budget, 2, CO2 column from differential absorption of reflected sunlight in the 1.61 μm band of CO2, J. Geophys. Res. Atmos., 107, ACH 6-1-ACH 6-16, http://doi:10.1029/2001JD000617, 2002.

415   Oda, T. and Maksyutov, S.: A very high-resolution (1 km? 1 km) global fossil fuel CO2 emission inventory derived using a point source database and satellite observations of nighttime lights, Atmos. Chem. Phys., 11, 543, http://doi:10.5194/acp-11-543-2011, 2011.

O'Dell, C., Connor, B., Bösch, H., O'Brien, D., Frankenberg, C., Castano, R., Christi, M., Fisher, B., Gunson, M., McDuffie, J., Miller, C. E., Natraj, V., Oyafuso, F., Polonsky, I., Smyth, M., Taylor, T., Toon, G. C., Wennberg, P. O., and Wunch,

420   D.: The ACOS CO2 retrieval algorithm-Part 1: Description and validation against synthetic observations, Atmos. Meas. Tech., 5, 99, http://doi:10.5194/amt-5-99-2012, 2012.

O'Shea, S., Bauguitte, S.-B., Gallagher, M., Lowry, D., and Percival, C.: Development of a cavity enhanced absorption spectrometer for airborne measurements of CH4 and CO2, Atmos. Meas. Tech., 6, http://doi:10.5194/amt-6-1095-2013, 2013.

425   Pachauri, R. K., Allen, M. R., Barros, V. R., Broome, J., Cramer, W., Christ, R., Church, J. A., Clarke, L., Dahe, Q., and Dasgupta, P.: Climate change 2014: synthesis report. Contribution of Working Groups I, II and III to the fifth assessment report of the Intergovernmental Panel on Climate Change, 151, 2014.

Palmer, P. I., Parrington, M., Lee, J. D., Lewis, A., Rickard, A., Bernath, P. F., Duck, T., Waugh, D., Tarasick, D., and Andrews, S.: Quantifying the impact of BOReal forest fires on Tropospheric oxidants over the Atlantic using Aircraft and Satellites

430   (BORTAS) experiment: design, execution and science overview, Atmos. Chem. Phys., 13, http://doi:10.5194/acp-13-6239-2013, 2013.

Pei-Tao, Z., Yin-Chao, Z., Lian, W., Yue-Feng, Z., Jia, S., Xin, F., Kai-Fa, C., Jun, X., and Xiao-Yong, D.: Analysis of influence of atmosphere extinction to Raman lidar monitoring CO2 concentration profile, Chin. Phys., 16, 2486, http://doi:10.1088/1009-1963/16/8/055, 2007.

435 Peters, W., Jacobson, A. R., Sweeney, C., Andrews, A. E., Conway, T. J., Masarie, K., Miller, J. B., Bruhwiler, L. M., Pétron, G., Hirsch, A. I., Worthy, D. E. J., Werf, G. R. v. d., Randerson, J. T., Wennberg, P. O., Krol, M. C., and Tans, P. P.: An atmospheric perspective on North American carbon dioxide exchange: CarbonTracker, Proc. Natl. Acad. Sci., 104, 18925-18930, http://doi:10.1073/pnas.0708986104, 2007.

Qi, C., Wu, C., Hu, X., Xu, H., Lee, L., Zhou, F., Gu, M., Yang, T., Shao, C., and Yang, Z.: High spectral infrared atmospheric
440   sounder (HIRAS): system overview and on-orbit performance assessment, IEEE Trans. Geosci. Remote Sens., doi: 10.1109/TGRS.2019.2963085, 2020. http://doi:10.1109/TGRS.2019.2963085, 2020.

Randerson, J., van der Werf, G., Giglio, L., Collatz, G., and Kasibhatla, P.: Global Fire Emissions Database, Version 4,(GFEDv4), ORNL DAAC, Oak Ridge, Tennessee, USA. https://doi.org/10.3334/ORNLDAAC/1293, 2015.

Rayner, P. and O'Brien, D.: The utility of remotely sensed CO2 concentration data in surface source inversions, Geophys. Res.
445   Lett., 28, 175-178, http://doi:10.1029/2000GL011912, 2001.

Rodgers, C. D. and Connor, B. J.: Intercomparison of remote sounding instruments, J. Geophys. Res. Atmos., 108, http://doi:10.1029/2002JD002299, 2003.

Takahashi, T., Sutherland, S. C., Wanninkhof, R., Sweeney, C., Feely, R. A., Chipman, D. W., Hales, B., Friederich, G., Chavez, F., Sabine, C., Watson, A., C.E.Bakker, D., Schuster, U., Metzl, N., Yoshikawa-Inoue, H., Ishii, M., Midorikawa,
450   T., Nojiri, Y., Körtzinger, A., Steinhoff, T., Hoppema, M., Olafsson, J., S.Arnarson, T., Tilbrook, B., Johannessen, T., Olsen, A., Bellerby, R., C.S.Wong, Delille, B., N.R.Bates, and Baar, H. J. W. d.: Climatological mean and decadal change in surface ocean pCO2, and net sea–air CO2 flux over the global oceans, Deep Sea Res. Part 2 Top. Stud. Oceanogr., 56, 554-577, http://doi:10.1016/j.dsr2.2008.12.009, 2009.

Wofsy, S. C.: HIAPER Pole-to-Pole Observations (HIPPO): fine-grained, global-scale measurements of climatically important
455   atmospheric gases and aerosols, Philos. Trans. Royal Soc. A, 369, 2073-2086, http://doi:10.1098/rsta.2010.0313, 2011.

Wunch, D., Toon, G. C., Blavier, J.-F. L., Washenfelder, R. A., Notholt, J., Connor, B. J., Griffith, D. W., Sherlock, V., and Wennberg, P. O.: The total carbon column observing network, Philos. Trans. Royal Soc. A, 369, 2087-2112, http://doi:doi.org/10.1098/rsta.2010.0240, 2011.

Wunch, D., Toon, G. C., Wennberg, P. O., Wofsy, S. C., Stephens, R. S., Fischer, M. K., Uchino, O., Abshire, J., Bernath, P.,
460   Biraud, S. C., Blavier, J.-F. L., Boone, C., Bowman, K. P., Browell, E. V., Campos, T., Connor, B. J., Daube, B. C., Deutscher, N. M., Diao, M., Elkins, J. W., Gerbig, C., Gottlieb, E., Griffith, D. W. T., Hurst, D. F., Jiménez, R., KeppelAleks, G., Kort, E. A., Macatangay, R., Machida, T., Matsueda, H., Moore, F., Morino, I., Park, S., Robinson, J., Roehl, C. M., Sawa, Y., Sherlock, V., Sweeney, C., Tanaka, T., and Zondlo, M. A.: Calibration of the Total Carbon Column

15

Observing Network using aircraft profile data, Atmos. Meas. Tech., doi: 10.5194/amt-3-1351-2010, 2010.
465 http://doi:10.5194/amt-3-1351-2010, 2010.

Wunch, D., Wennberg, P. O., Osterman, G., Fisher, B., Naylor, B., Roehl, C. M., O'Dell, C., Mandrake, L., Viatte, C., and Kiel, M.: Comparisons of the Orbiting Carbon Observatory-2 (OCO-2) X CO2 measurements with TCCON, Atmos. Meas. Tech., doi: 10.5194/amt-10-2209-2017, 2017. http://doi:10.5194/amt-10-2209-2017, 2017.

Yang, Z., Bi, Y.-M., Wang, Q., Liu, C.-B., Gu, S.-Y., Zheng, Y., Lin, C., Yin, Z., and Tian, L.: Inflight Performance of the
470 TanSat Atmospheric Carbon Dioxide Grating Spectrometer, IEEE Trans. Geosci. Remote Sens., http://doi:10.1109/TGRS.2020.2966113. 2020.

Yang, Z., Zhen, Y., Yin, Z., Lin, C., Bi, Y., Liu, W., Wang, Q., Wang, L., Gu, S., and Tian, L.: Prelaunch radiometric calibration of the tansat atmospheric carbon dioxide grating spectrometer, IEEE Trans. Geosci. Remote Sens., 56, 4225-4233, http://doi:10.1109/TGRS.2018.2829224, 2018.

475 Yao, B., Huang, J., Zhou, L., Fang, S., Liu, L., Xia, L., Li, P., and Wang, H.: Preparation of mixed standards for high accuracy CO2/CH4/CO measurements., Environ. Chem., 02, 135-140, http://doi:10.7524/j.issn.0254-6108.2013.02.019, 2013.

Yevich, R. and Logan, J. A.: An assessment of biofuel use and burning of agricultural waste in the developing world, Global. biogeochem. cycles., 17, http://doi:10.1029/2002GB001952, 2003.
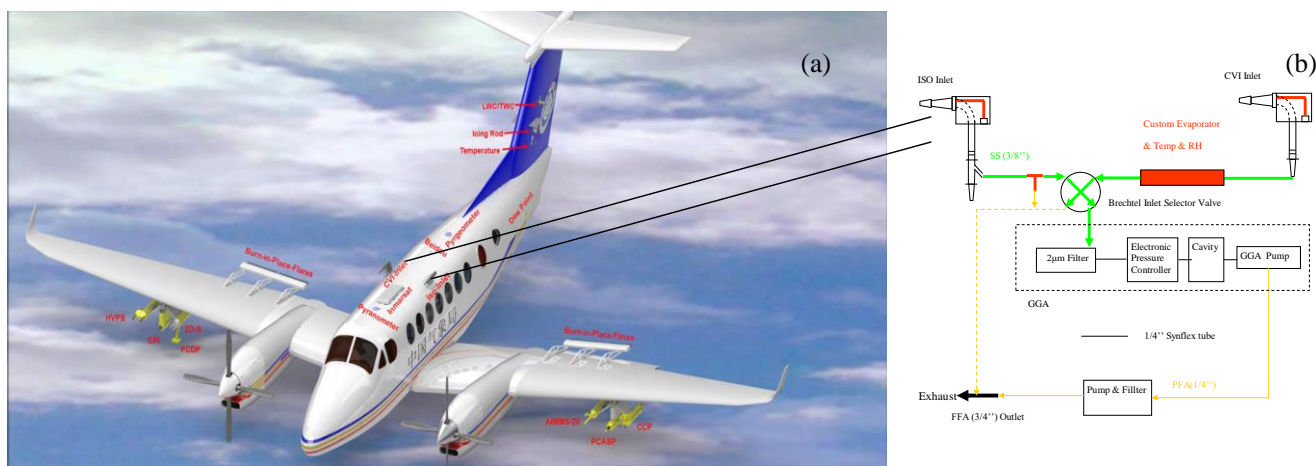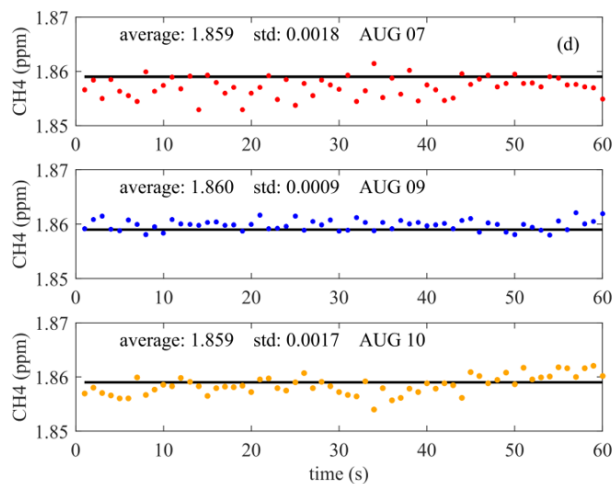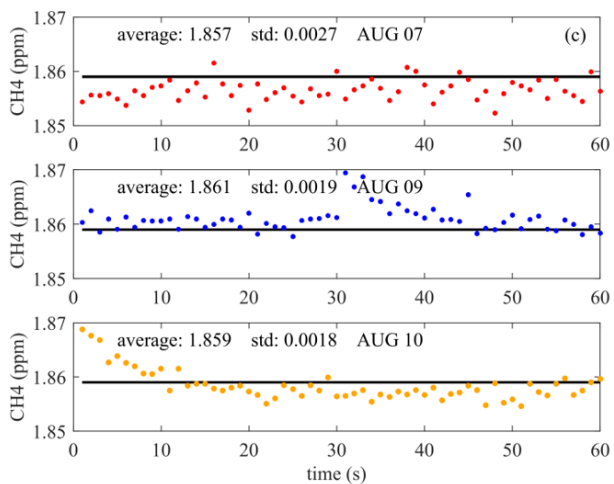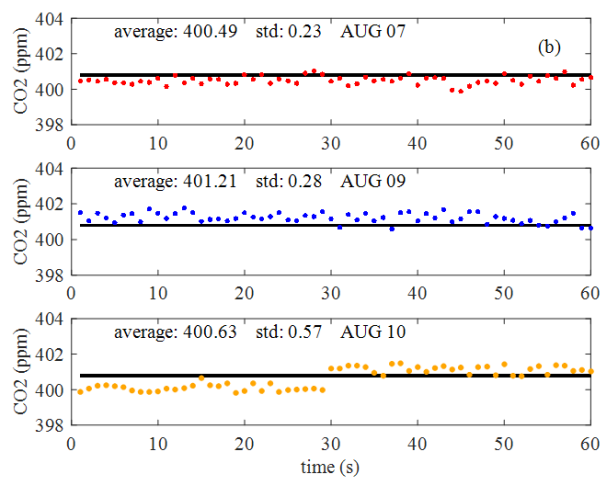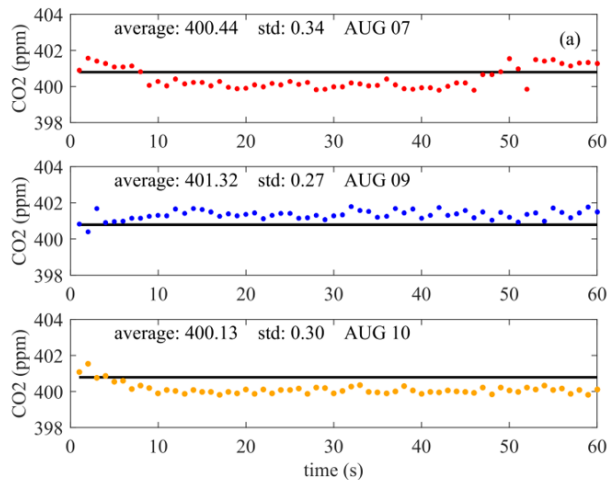
480

Figure 1. ~~Observation area for aircraft-based measurement of CO2 and CH4 over Jiansanjiang, Northeast China.~~ (a) The outside view of the Beechcraft King Air 350ER instrumentation. (b) The schematic diagram of the greenhouse gases sample airflow.

Figure 2. ~~Trajectory of the August 7 flight in Jiansanjiang. The color scale shows the progression of time in local time, where blue represents the start time of the data profile, and red represents the end time.~~ The concentration of CO_2 (a) and CH4 (b) before the flight, and the concentration of CO_2 (a) and CH4 (b) after the flight obtained during the calibration, with the value of standard deviation and average of each calibration.
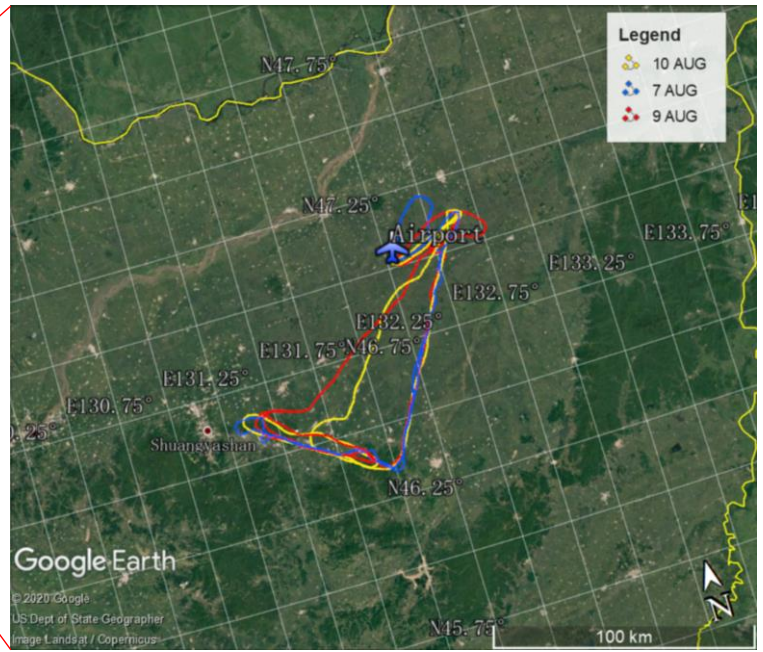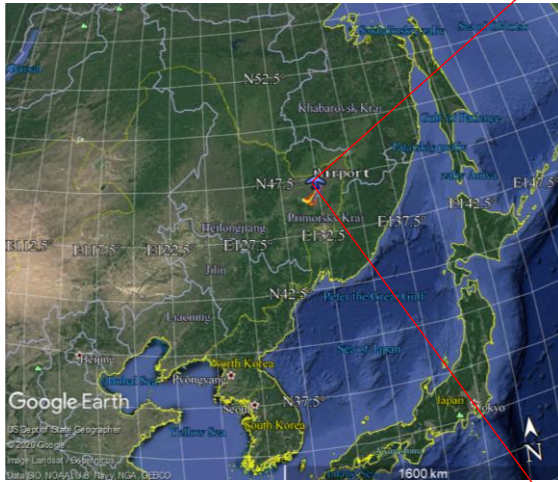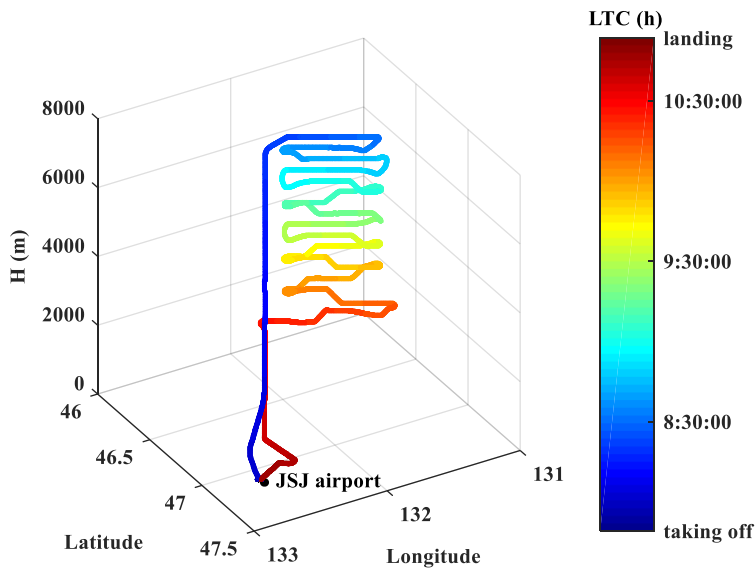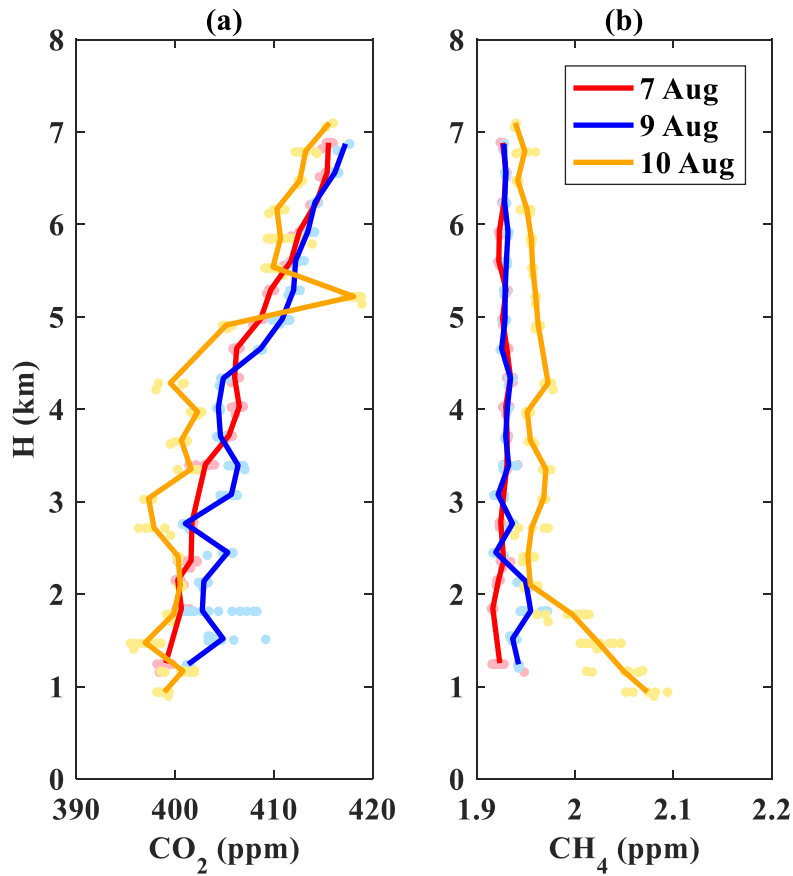
485

490

17

Figure 3. ~~Vertical profiles of (a) CO2 and (b) CH4 observed on August 7 (blue), 9 (red), and 10 (yellow), 2018, over Jiansanjiang measured in situ with aircraft. The aircraft-based in situ measurement data are indicated with dots, and averaged data for each flat flight stage are shown as lines.~~ Observation area for aircraft-based measurement of CO_2 and CH4 over Jiansanjiang, Northeast China, and the flight paths on 7, 9, 10 August.

Figure 54. Comparison of aircraft measurements (in situ measurement data are shown as circles, and averaged data for each flat flight stage is indicated by the red line) collected on August (a) 7, (b) 9, and (c) 10, Tan-Tracker (v1) data (blue line) at the location of Jiansanjiang linearly interpolated to the observation times on August (a) 7, (b) 9, and (c) 10, and the OCO-2 averaged profile (gray line) for the aircraft flight area from August 5 with 1 standard deviation (gray bars). Vertical profiles of (a) CO_2 and (b) CH4 observed on August 7 (blue), 9 (red), and 10 (yellow), 2018, over Jiansanjiang measured in situ with aircraft. The aircraft-based in situ measurement data are indicated with dots, and averaged data for each flat flight stage are shown as lines.
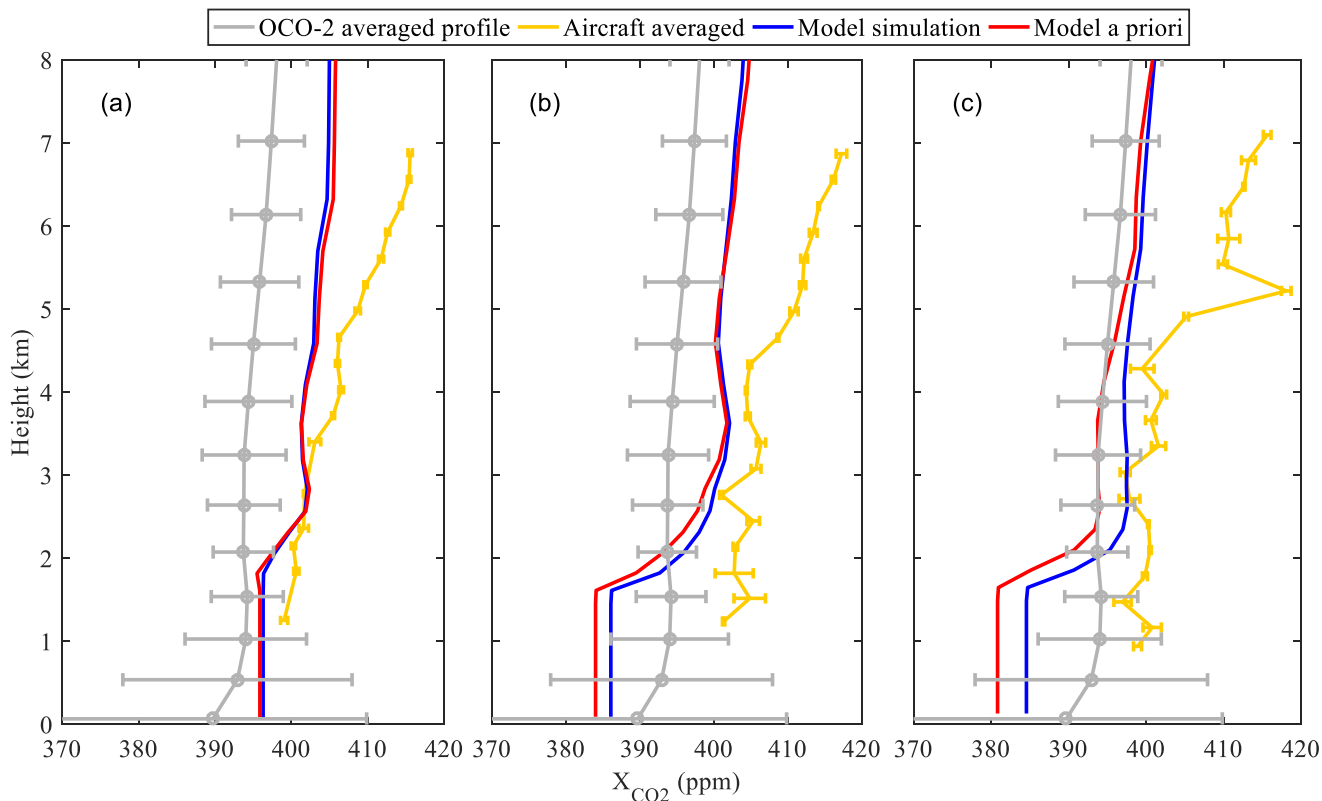
Figure 65. ~~Extrapolated CO2 profiles observed on August 7, 9, and 10, 2018, over Jiansanjiang. Red, blue, and yellow solid lines show the aircraft-based (in situ) data collected on August 7, 9, and 10, respectively, averaged for each flat stage of the flight. Dotted lines show the extrapolated parts of the profiles, with colors corresponding to sampling dates in accordance with the solid lines. Black horizontal lines show the tropopause height from NCEP reanalysis data.~~ Comparison of aircraft measurements (in situ measurement data are shown by the yellow line) with 1 standard deviation (yellow bars) collected on August (a) 7, (b) 9, and (c) 10, Tan-Tracker (v1) data (blue line) and the a priori profile of it (red line) at the location of Jiansanjiang linearly interpolated to the observation times on August (a) 7, (b) 9, and (c) 10, and the OCO-2 averaged profile (gray line) for the aircraft flight area from August 5 with 1 standard deviation (grey bars).
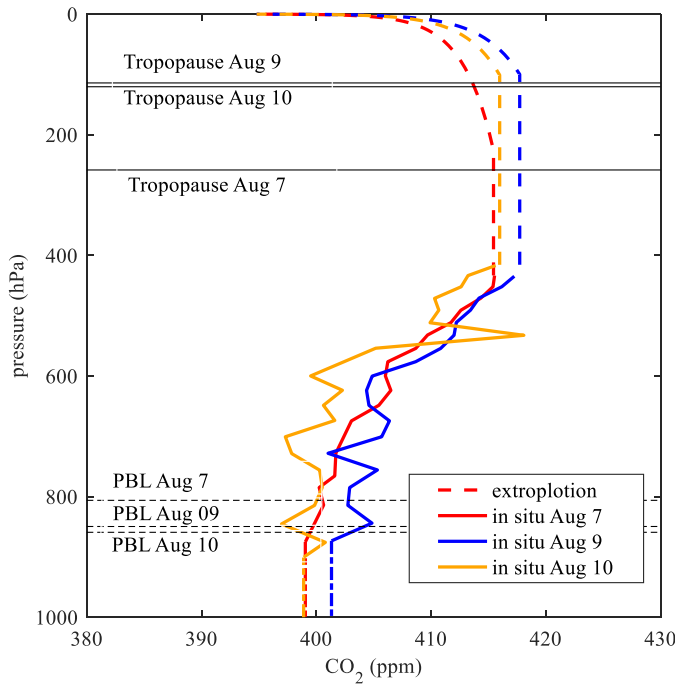
510

515

20

Figure 7. Extrapolated CO_2 profiles observed on 7, 9 and 10 August, 2018, over Jiansanjiang by method (2). Red, blue, and yellow solid lines show the aircraft-based (in situ) data collected on 7, 9 and 10 August, respectively, averaged for each flat stage of the flight. Dotted lines show the extrapolated parts of the profiles, with colors corresponding to sampling dates in accordance with the solid lines. Black horizontal lines show the tropopause height from NCEP reanalysis data.

Table 1 Details of the flight on each day.

Date	Flight Time (LTC)	Fight Altitude (m)
7 August, 2018	07:49:08-10:53:32	59-7205
August 9, 2018	07:50:19-10:45:57	61-7190
August 10, 2018	07:56:02-10:54:11	65-7104

Table 2~~1~~. X_{CO2}~~XCO2~~ derived from aircraft on each observation day (~~August 7, 9, and 10~~7, 9 and 10 August) supplemented the aircraft profile by method (1). OCO-2 (V9r) X_{CO2}~~XCO2~~ were from August 5, which was the closest time point of X_{CO2}~~XCO2~~ data from OCO-2 over Jiansanjiang to the observation period. Differences between aircraft X_{CO2}~~XCO2~~ and OCO-2 are shown in the fourth (ppm) and fifth (%) columns. The average difference and standard deviation are shown in the fifth row.

Date	Aircraft* (ppm)	OCO-2 (ppm)	Difference (ppm)	$\dfrac{\text{OCO-2-Aircraft}}{\text{Aircraft}} \cdot 100\%$ (%)
~~August 7~~7 August, 2018	~~398.33~~401.95	396.91	~~-1.42~~-5.04	~~-0.35~~-1.27

21

August 9, 2018	401.62401.72		=4.71 4.81	=1.17 1.21
August 10, 2018	397.95401.10		=1.04 4.19	=0.26 1.06
		Average (1σ)	=2.39 (2.02) 4.68(0.44)	=0.59 (0.44) 1.18(0.11)

*The effect of the average kernel was taken into consideration for OCO-2.

Table 2 The same as Table 2, but for method (2).

Date	Aircraft* (ppm)	OCO-2 (ppm)	Difference (ppm)	$\dfrac{\text{OCO-2-Aircraft}}{\text{Aircraft}} \cdot 100\%$ (%)
7 August, 2018	401.54		-4.63	−1.16
August 9, 2018	403.45	396.91	−6.54	−1.64
August 10, 2018	401.02		−4.11	−1.03
		Average (1σ)	−5.09 (1.28)	−1.28 (0.32)

Table 32. Aircraft integration error budget of X_{CO_2} estimation for method (2). Errors in the three profiles from multiple error sources contributed to the calculation results of the integrated total column. The error is spilt into four sources, similar to previously described error budgets (Wunch et al., 2017): the contribution from the aircraft profile itself, the contribution from the unknown surface to the bottom of the profile, the contribution from the upper troposphere and stratosphere, and error from the tropopause height.

Date	PBL error (ppm)	Upper troposphere and stratosphere error (ppm)	Tropopause height error (ppm)
August 77 August, 2018	0.060.086	0.290.323	0.660.054
August 9, 2018	0.060.076	0.340.303	0.030.017
August 10, 2018	0.070.077	0.280.077	0.010.017
Average (1σ)	0.060.079	0.300.234	0.230.029

<u>**Response to Comments of reviewer 1**</u>

The authors thank all reviewers for their constructive comments and suggestions, which have helped us to improve the quality of this paper both in sciences and writing. All comments are carefully considered and responded. The response in blue italic letters follow each comments in black.

1. General comments:

    The paper by Sun et al. reports from airborne in-situ measurements over North-East China in August 2018. The in-situ profiles derived on three different days are compared with profiles from OCO-2 and a carbon cycle data assimilation data system (Tan-tracker). The topic of the manuscript is of high importance since high-quality observations are needed to enable a better analysis of the global carbon cycle. Specifically, in-situ measurements are highly valuable to study local phenomena in detail and to allow for an evaluation of satellite products. This is especially true and important for regions were observations are rare and the variability of the atmospheric greenhouses are not well constrained, because emission amounts are not well known. Therefore I strongly encourage the authors to continue their work in this field because the gained data sets are highly valuable to the carbon community. However, the manuscript lacks on a detailed description and discussion to support the conclusions drawn by the authors. Personally, I also doubt the quality of the aircraft borne in-situ measurements and therefore suggest publication of the manuscript only after my main (specific) comments are carefully addressed.

    Specific comments:

    I suggest to re-structure the manuscript and to expand the section "instrumentation" to "methods" by including a subsection on Tan-Tracker and OCO-2 (including a thorough description of the model products and the derivation of the OCO-2 data product).

Thank you so much for the advice on this study. The section 2 "Instruments" is rewritten as "Methods" and the original context of section 2 changed to 2.1 "Aircraft Instrumentation". In addition, we added section 2.2 "Tan-Tracker and OCO-2 data" to describe the Tan-Tracker (v1) model and the OCO-2 data used in this article, please see detail in section 2.2, Page 5, Line 135 in the revised manuscript:

"Based on the nonlinear least squares four-dimensional variational data assimilation algorithm (NLS-4DVar) and the Goddard Earth Observing System atmospheric chemistry transport model (GEOS-Chem), Tan-Tracker provides surface flux inversion estimates and profiles of CO_2 with 47 levels of vertical

resolution from the surface to 0.03 hPa and horizontal resolution of 2.5° × 2°. The NLS-4DVar assimilation model Tan-Tracker (v1) and OCO-2 XCO2 (v9r) retrievals are used to optimize surface terrestrial ecosystem CO2 flux and ocean CO2 flux, while prior Fossil Fuel emission and prior Fire emission remain unchanged (details of model setting and prior flux information can be found in Han and Tian, 2019).

The Orbiting Carbon Observatory-2 (OCO-2), successfully launched on 2 July 2014, obtained global measurement of CO2 through hyperspectral measurement of reflected sun light from earth atmosphere in one NIR and two SWIR bands centre at 0.76, 1.61 and 2.06 μm, more details about the mission, retrieving algorithm and data characteristic can be found in Crisp et al. (2008) and O'Dell et al. (2012). The uncertainty and bias of the X_{CO2} products related to surface properties, aerosol and cloud, and the retrieving algorithm has been reported by Butz et al. (2009), Jung et al. (2016) and Connor et al. (2016). The OCO-2 data (V9r) including X_{CO2}, CO_2 profile and the a priori profile was used in this study.
"

2. Page 2, L41: all-weather?

Response: *We corrected the sentences in line 42, Page 2 as "… , which can provide global coverage of the column-averaged dry-air mole fraction of CO_2 (X_{CO2})"*

3. P3, L92: Which one? AIMMS-20?

Response: *Yes, we corrected the words "AIMMS" to "AIMMS-20AG" and we added following sentences after that (Line 95, Page 3):*
"The geolocation information including latitude, longitude, ambient pressure and height of the aircraft is also measured by AIMMS-20AG. The relative humidity is calculated by temperature and dew point, measured by the Total Temperature Sensor (Model 102 Type Non-De-iced, Rosemount Aerospace Inc) Dew Point Hygrometer (Model 137 Vigilant™, EdgeTech), respectively."

4. P3, L94: Why did you use a CVI inlet? Where there other measurement (aerosol) systems onboard? Please be also more specific w.r.t. to the airborne set-up. Did you need to use an external pump to achieve the large gas flow? How long was the inlet (from the tip to the cell)? I am not aware of a publication which reports the airborne deployment of this kind of analyzer, so I suggest to include a

schematic which shows the set-up and the periphery to control cell/inlet pressure, temperature and volume or mass flows.

Response: The aircraft is designed for weather modification by China Meteorological Administration (CMA), and with lucky, we are allowed to take our greenhouse gas analyzer aboard to carry on the measurement of CO2 and CH4. The infrastructure of the aircraft and the gas flow system is designed and fulfilled in USA by the team of weather modification. We loaded our greenhouse gas analyzer inside of the aircraft and modified some gas flow arrangements to better fit the requirement for greenhouse profile measurement. We use CVI inlet and/or the ISO inlet which had been installed on the aircraft. The ISO inlet was used when the aircraft passed through the cloud, and the CVI inlet was used at other time. The schematic diagram was shown in the figure 1 (in the revised manuscript). As the schematic diagram shows, the external oil-less diaphragm vacuum pump (F-9A 08-03, GAST) was mounted between the CVI inlet and/or the ISO inlet, with the maximum pressure of 31.15 l/min used to keep a stable airflow. The length of the air channel from the tip of the inlet to the cell is about 0.6 meters. The development of an airborne system for greenhouse measurement using the cavity-enhanced absorption spectroscopy technique (CEAS) has been reported by O'Shea et al. (2013) and Palmer et al., (2013).
The sentence is corrected in the revised manuscript in section 2.1, Line 99, Page 4:
"The ultraportable ... which consists of CVI (Model 1204; Brechtel Manufacturing Inc.) and ISO inlet (Model 1200; Brechtel Manufacturing Inc.) in the pressurized cabin for continuous measurement of CO_2 and CH_4."

5. P3, L96: SL/min? Which kind of Mass Flow controller?

Response: The air sample flow rate of CVI inlet is constant of 15 l/min (Aircraft-based Counterflow Virtual Impactor Inlet System CVI - Model 1204, Brochure).

The following sentences are added in the revised manuscript (Line 103, Pages 4)
"The CVI and/or ISO inlet was mounted on the top of the aircraft body as shown in figure 1, and the air flow rate of the inlet is kept constant by the automatic air flow controller of the inlet (Aircraft-based Counterflow Virtual Impactor Inlet System CVI - Model 1204, Brochure; Isokinetic Inlet System ISO Inlet - Model 1200, Brochure)."

6. P3, L97: The given values are from the manufacturer and might be valid for controlled laboratory conditions. Usually, the performance on a mobile platform is highly affected by variations of pressure, temperature and/or mechanical vibrations. I assume that this specific instrument is even more sensitive since it is not especially designed for use aboard research aircraft. Did you cross-check the theoretical precision values yourself in the laboratory, e.g. by supplying the system with sample gas of constant CO2 and CH4 mixing ratios? Did you check the sensitivity of your instrument to changes in pressure and temperature? Did you check the short and long-term drift of your instrument's sensitivity (i.e. over one flight and over a couple of days, respectively)? Did you check the repeatability of your measurements?

Response: Just before taking off, the Greenhouse Gas Analyzer (GGA) was calibrated against the standard gas, and the stability of instrument was checked and tested, immediately after touching down, again the same standard gas of CO2 and CH4. The data obtained after the calibration process are shown in figure 2 in the revised manuscript, it shows a relatively stable measurement and without drift after the flight.
The precision and reparability of the instruments are also checked and test multiple times in the laboratory and the results show that it is stable and good for the measurements. Please see more details about the standard gas and the calibration process in response 10.

7. Comment: P3, L98: What do you mean with response time in this case? Is this the response time of the system to a change in atmospheric concentrations (due to e.g. the residence time in the inlet)? Is it the averaging time to achieve the given precision (in theory)? O is it the flush time of the cell and thus, gives the best achievable time resolution?

Response: The response time in this place means the averaging time to achieve the given precision, and the data processing was made to smooth with a 10-s running average to further remove errors. The residence time in the inlet from the tip to the analyzer of the system is around 220 seconds, and the data during this period in each level flight are removed (which means only the data 220 seconds after the flight keeps level are used) and reanalyzed, the modified results and figure are given in the revised manual .

The following sentences are added in revised manuscript (Line 106, Page 4)
"The UGGA uses a cavity ringdown absorption technology, called off-axis integrated cavity output

spectroscopy, to determine the trace gas concentration with a high precision of < 300 ppb (CO2) and < 2 ppb (CH4) and a 10-s response time according to the user manual and was tested and controlled in the laboratory."

8. P3, L98: Please specify: Where was the pressure controller installed? I assume in front of the instrument? How constant was the pressure during the flight?

Response: As the schematic diagram shows, the external oil-less diaphragm vacuum pump (F-9A 08-03, GAST) was mounted between the CVI inlet and/or the ISO inlet, with the maximum pressure of 31.15 l/min used to keep a stable airflow. There is also a smaller pump inside the UGGA system to exhaust air outside the analyzer to the outlet tube and the maximum flow of the pump of UGGA is about 0.3 l/min so the pressure and the air flow to the UGGA can be controlled. We add the cell pressure of the instrument cavity as the supplement figure 1, which shows that the pressure is stable in each level flight. The standard deviation of 0.029, 0.029, 0.033 and the range of the cell pressure of three flights is 51.31-51.43 torr, 51.32-51.43 torr, 51.30-51.42 torr on 7 August, 9 August and 10 August.

Explanation is added in the revised manuscript (Line 116, Page 4):
"The sample cavity temperature was also kept stable and constant by the temperature controller of the instrument. The instrument automatically recorded and saved the temperature and pressure in the cavity during operation. According to the records, the standard deviation of the cell pressure during three flights is 0.029, 0.029, 0.033 on 7, 9 and 10 August and the range of the cell pressure on each flight is below 0.12 torr."

9. P3, L99: Which temperature? The cell temperature? A range of more than 6 degrees seems very huge to me and should impact the sensitivity of the instrument. Did you check this in the lab (see also above)?

Response: Yes, it is the cell temperature, and we added supplement figure 2 shown the cell temperature with height. Considering the large variation of the cell temperature which may reduce the precision of the instrument, only data when cell temperature is within 3-sigma is used in analyses, with the range of cell temperature, respectively for the three flights, between 28.85-29.69°C, 28.26-31.37°C, 29.09-31.43°C, the standard deviation of 0.46 (7 August), 1.55 (9 August), 1.18 (10 August).

We corrected the sentences in our manuscript, Line 115, Page 4 to:

"The sample cavity temperature are also remain stable and constant by the temperature controller of the instrument."

And we added the sentence in our manuscripts, Line 118, Page 4:

"For the cell temperature, the standard deviation is 0.46, 1.55 and 1.18 on each day and the range of it is below 3.11℃."

10. P3, L99: Please provide more details on the Standards. How many standards did you use? At which concentrations? How did you calibrate the system? Did you (or some of the other institutions cross-calibrate the standards in a way that they are traceable to the typically used NIST standards? How stable was the system? How reproducible were the standard measurements before and after the flight?

Response: We added some details on the standards, and explanation is added in the revised manuscript, Line 123, Page 4:

"The standard gas we used is based on dry and clean air with greenhouse gases known concentration value, filled in a 29.5L aluminum alloy cylinder with silanization and other special treatment on the inner wall, traceable to the world meteorological organization global atmospheric observation network (WMO-GAW) level 1 standard gas. The concentration of the CO_2 is 400.13 ppm and CH_4 is 1.867 ppm. The standard gas we use has been measured in the laboratory for the proportion of $\delta13C$ in CO_2. The range of the proportion is -8.0‰ to -8.2‰ close to the natural content, so it will not cause significant isotopic effect on the measurement of CO_2 by optical method and meet the requirements of standard gas (Yao et al., 2013). Just before taking off, UGGA was calibrated against standard gas, and the stability of instrument was checked and tested again using the same standard gas of CO_2 and CH_4 immediately after landing. As shown in Figure 2, the concentration of CO_2 and CH_4 before and after landing is stable around the value of standard has concentration, and there is almost no drift after the flight. The precision and reparability of the instruments are also checked and test multiple times in laboratory and the results show that it is stable and good for the measurements."

11. P4, L107, Figure 1: What do you want to show with this figure? I suggest to zoom in and to include at least the flight patterns of all 3 flights conducted in August 2017. You might also show a series of three figures with all three flight paths plotted over a weather map.

Response: We revised figure 1 (figure 3 in the revised manuscript) which shows the large area including the experiment site and the airport by google map and zooms in with flight path shown on the map. Because after taking off, the aircraft climbed up directly to the maximum height, only the paths in the decline phase are plotted to better display level flight trajectory, and only measurement during level flight are used for analysis. The flight paths for the three days is similar, so only the trajectories on 7 August is given in the article, and the flight path on 9 and 10 August aircraft are given in the supplement, we added in supplement figure 3 .

We corrected the sentences in our manuscript, Line 149, Page 5 to:
"Aircraft measurement were carried out from 7 to 10 August over Jiansanjiang (47.11°N, 132.66°E, 61 m above sea level), located in Heilongjiang province, Northeast China. Figure 3 shows the geolocation of the Jiansanjiang aircraft and the fight path."

12. Section 3: This section is especially weak. I suggest to include information about the flight strategy, as well.

Response: Thanks for the advice, we rewrite section 3, and added more sentences about the flight strategy, and explanations are added, please see response to next comment.

13. So e.g., why did you fly in in the morning hours (during which the boundary layer develops)? Did you try to match the time of an OCO-2 overflight? Or was this due to logistical (ATC) reasons? Why did you choose to fly over a horizontal distance of 150 km (the swath is a couple of km´s only)? Did you adjust the flight track to measure along-track of OCO-2? Or is this Did you always follow the same flight strategy on the three days? What was the descending rate and the corresponding pressure variation during spiraling down?

Response: The flight strategy was added and explained, and we added table 1 listed the details of the three flights. Since we cannot decide when to fly since the ATC restriction to avoid the civil aviation, so that we did not adjust the flight track to measure along-track OCO-2.

Explanation as following is added in the revised manuscript, Line 155, Page 5:
  "The aircraft is designed for weather modification by China Meteorological Administration (CMA), so

14. P4, L110, Figure 2: From this figure it looks like that you did ~7 constant flight legs, is that correct? I don´t think you need this figure if you provide a horizontal map of the flight patterns as suggested for figure 1, which gives an idea about the flight dimensions in Lat/Lon direction. Instead, I suggest to include a simple time-series of in-situ measured CO2, CH4, and flight altitude for this particular flight.

According to figure 3, the flight trajectory in 7 August looks like that there are about 7 level flights in this flight, and the level flight is about every 300-700 m during the flight as the figure shows. From figure 3 we want to show the horizontal coverage of these flight and the flight trajectory, since the 3-D figure may not necessary in all three days which looks identical, and we added the flight trajectory of the other two days (9 and 10 August) shown in the supplement figure 3. The horizontal map overlaid with the flight trajectory in three days (7, 9, 10 August) is shown in figure 4 (in the revised manuscript), which we have revised the original one, and we hope these figures can look better which gives the idea of the dimensions of the flight pattern with relative information of the surface. And the variation of mole fraction of CO2, CH4 with flight altitude in the flights are shown in figure 5 (in the revised manuscript).

__Response:__ We corrected the sentences and more explanations as following are added in the revised manuscript to make it clear. Line 165, Page 6:

"The flight trajectory on 7 August is shown in figure 4. The aircraft climbed up quickly and directly to the maximum height to about 7.5 km 30 min after taking off, and then descending down step by step at about every 300 m. Since the 3-D figure in these three days looks identical, the flight trajectory of the other two days (9 and 10 August) is not shown in figure 4."

And also we put the information of airport Jiansanjiang and flight trajectory in the newly plotted figure 3.

15. Section 4: Please keep in mind that there are several ways how variable water vapor levels influence the CO2/CH4 measurements: 1) The dilution effect, 2) variation in the line broadening of the carbon dioxide and methane lines due to varying water vapor concentration, and 3) nonlinearity of the reported water vapor concentration due to self-broadening of the water vapor line. Here you discuss the dilution effect which certainly is the most important one. However, the water concentration measurement must be highly accurate to allow for a meaningful accuracy in the derived dry gas concentrations. Therefore, I´d like to see an in-depth error analysis for the approach used herein. Moreover, I suggest to include the time-series of measured relative humidity and derived water vapor (including error bars!), at least in the supplement.

Response: The measurement is making under real humidity conditions, so the water vapor had to be corrected to drive the CO2 and CH4 concentrations under dry conditions. We find that the measured relative humidity and temperature by AIMMS-20AG may have some uncertainty, so we used the static temperature measured by the Total Temperature Sensor (Model 102 Type Non-De-iced) and the dew point temperature measured by Dew Point Hygrometer (Model 137 Vigilant™, EdgeTech). To estimate the ambient humidity, we calculated the relative humidity by the dew point and temperature, and then doing water correction of CO2 and CH4 mixing ratio.

We have no corresponding facilities to measure the measure the broadening effect of water vapor on the spectral line, we suppose the instrument factory have considered this effect during factory calibration experimental, so the water vapor correction except for dilution was not considered here. The RH profile we added in supplement figure 4 (a) with 1-σ uncertainty bar, and the data is accurately time- matched to the CO2 and CH4 profiles. We also added the ambient temperature and pressure during the flight in supplement figure 4 (b) and (c), respectively. Time-series of measured pressure, dew point and temperature are given in the supplement figure 5. The processing process of is the same as that of CO2 and CH4. The 1-σ of the data in the level flight is taken as the uncertainty, their variation with height are also shown in the figure.

Corrections and explanation are added in the revised manuscript, Line 184, Page 6:

"Where $L_v = 2.500 \times 10^6$ J Kg^{-1}, M_w is the molecular weight of water equals to 18.016, R = 8.3145 J K^{-}

16. P5, L 132: All data are recorded at 1s and then smoothed to remove errors because of the response time? As mentioned above, please be clear in the use of your wording w.r.t. response time. The residence time usually can be corrected for if e.g. volume flow and inlet pressure are known.

***Response:** Yes, the measurement are made at 1s frequency and then 10-s average are done to smooth and remove potential errors concerning the response time. Concerning the residence time of air flowing the pipe and cell. We have modified the data processing method to take the effect of gas residence time in the pipeline into account. Therefore, we removed the data 220s from the start during the level flight in average, because this data was acquired during the descent of the aircraft, which may cause uncertainty of the measurement.*

Corrections as following are added in the revised manuscript, Line 197, Page 7:
"The time points at the beginning and end of level flight are determined according to the altitude and its variation of the aircraft. Considering the residual time of the GHG measurement system, the data obtained 220s from the start of the level flight is considered to be observed when the aircraft is descending rather than in level, which may cause uncertainty of the measurement. Therefore, the data were reserved after the level flight starting for 220s. If the duration time of certain level flight lasted less than 220 s, the data observed during that level flight were also discarded."

17. Section 5, Figure 3: This figure shows that you did much more constant flight legs than it seems from figure 2. Do these dots represent 10s values? What is real variability and what is instrument precision? Variation in CO2 on each leg is large (maybe also because of the large horizontal distance), the vertical variability on Aug 10 seems larger than the horizontal variability on that day. Is this a real atmospheric feature and do you have any explanation for this? Also, the boundary layer variability on 9 Aug seems much larger than on other days. Is this a horizontal gradient? Please include a more indepth discussion on these profiles. I´d like to also see the standard deviation or even better, median

instead of average values including some percentiles. What was the boundary layer height? Please include also a vertical profile of met. variables, at least in the supplement.

Response: Please see the response to the previous comment about the data processing.

We corrected the figure 3 as the reason mention in response to the previous comment, (figure 5 in the revised manuscript), the lines represent the average value of each level flight and the dots represent the data obtained after the 10s average, water correction and the residual time correction. The 1-σ bars are given in the figure 6 in the revised manuscript. Since only the data during the level flight are analyzed, the data during landing time was discarded, which is about from 1 km to the surface, and it is difficult for us to correctly estimate the boundary layer height based on the observation data obtained by the aircraft. The meteorology data are given in the supplement. time-series of temperature and dew point is shown in supplement figure 5, and the profile of RH, temperature and pressure is shown in supplement figure 4 (a), figure 4 (b), figure 4 (c), and the meteorology data are accurately time-matched with that of CO2 and CH4 data.

18. P5, L 142: "was attributed to different weather conditions": Please provide more details on this hypothesis.

Response: The weather condition during the three flights are sunny, overcast and overcast on 7, 9 and 10 August respectively, as the sentences in P5, L143 indicated, so we assume that the relatively larger gradient of the CO2 profile from around 0.6 to 2 km on 7 August might be caused by the weaker CO2 uptake from the vegetation on the surface.

We corrected the sentence (Line 216, Page7) as "… was probably attributed to different weather conditions…"

19. P6, L161: Please give a short introduction about the Model, the used a-priori information and the simulations – and the difference. Which data are assimilated? The OCO-2 data? Doesn´t look like. The aircraft data?

Response: Tan-Tracker (v1) is a 4D-Var assimilation model and OCO-2 XCO2 retrievals (v9r) are used to optimize surface terrestrial ecosystem flux and ocean flux, with prior Fossil Fuel emission and prior

Fire emission remain unchanged. Carbon Tracker posterior flux (v2017, Peters et al., 2007, https://www.esrl.noaa.gov/gmd/ ccgg/carbontracker/) was used as prior terrestrial ecosystem CO_2 flux and scaled ocean flux (Takahashi et al., 2009, scaled to 2016 with Marine Boundary Layer CO_2 concentration www.esrl.noaa.gov/gmd/ccgg/GHGreference/) was used as prior ocean flux in Tan-Tracker (v1). Prior Fossil Fuel emission including fossil fuel emission of Open-source Data Inventory of Anthropogenic CO_2 (ODIAC) (Oda and Maksyutov, 2011, http://www.odiac.org/index.html), ship emission (Endresen et al., 2007) and aviation emission of Aviation Emissions Inventory Code (AEIC) (scaled to 2016, Olsen et al., 2013). Prior Fire emission including biomass burning emission of Global Fire Emissions Database v4 (GFED4) (Randerson et al., 2018, http://www. globalfiredata.org/index.html) and biofuel emission (Yevich and Logan, 2003). The above described prior fluxes used to drive GEOS-Chem for the CO_2 simulation were integrated and provided by the Harvard–NASA Emissions Component (HEMCO) model (Keller et al., 2014). Model a priori and model simulation used in our manuscript are GEOS-Chem simulation forced by prior flux and Tan-Tracker (v1) results separately.

Note that prior terrestrial ecosystem flux and ocean flux are different from those used in observing system simulation experiments (OSSEs) of Han and Tian (2019). But their description of OCO-2 data assimilation experiment is still in writing, so we only cite Han and Tian (2019).

We add follow sentences in the newly added section 2.2, Line 148, Page 5, as mentioned before:

"The NLS-4Dvar assimilation model Tan-Tracker (v1) and OCO-2 XCO2 (v9r) retrievals are used to optimize surface terrestrial ecosystem CO_2 flux and ocean CO_2 flux, while prior Fossil Fuel emission and prior Fire emission remain unchanged (details of model setting and prior flux information can be found in Han and Tian, 2019)."

20. P6, L 163: "The variation of CO2 ….". I don´t understand this sentence. Do you talk about the aircraft measurements? What about uncertainty bars for the aircraft data?

Response: *The variation here means the structure of CO2 vertical profile which can be divided into three parts according to different characteristic of variation. We corrected figure 4 (figure 6 in the revised manuscript) and added 1-σ bars. The sentence (Line 241. Page 8 in revised manuscript) are corrected to make it more clear:*

"The structure of CO_2 varied with height could be roughly divided into three segments: surface to 2 km, 2 to 3 km, and 3 to 8 km (Figure 6)."

21. P6, L165: Reproducing CO2 uptake from vegetation by a model is highly challenging, but I do not see any information from the model (neither a-priori or simulated). Is this what you mean with "Below 2km, CO2 is assumed to be vertically mixed…"?

Response: Because the model keep the same mole fraction of CO2 profile below 2 km, it cannot provide any information of the source and sink on the ground. The profile of the aircraft showed low concentration near ground and increased with the height, but currently the model did not reflect this feature. And we added the explanation about it in Line 254, Page 9, as mentioned in the responds to specific comments.

22. Comment: P6, L166: OCO-2 data were averaged over what area and what time? Please provide a graphical explanation which OCO2-Data you used. How did you get the vertical information?

Response: Because no data were obtained from OCO-2 over Jiansanjiang during the flight on 7, 9 and 10 August, we used the satellite data on 5 August which is closest in time to the experiment. The 1° × 1° average of the data were used for comparison. The height information of the satellite profile is available on the satellite products.
Correction and explanations as following are added in in the revised manuscript, Line 238, Page 8:
"Because no data were obtained from OCO-2 (v9r) …."

23. P6, L175: "…with large differences in values". So do you have any explanation? Apart from the quality of the in-situ data, one reason might be the comparison of measurements on different days. To get an impression about the day-to-day variability in that region, you might have a look at a longer timeseries of OCO-2 data. You also might have a look at the weather conditions (low or high pressure systems, frontal crossings) and how these may have influenced the day-to-day variability.

Response: Explanations as following are added in the revised manuscript, Line 254, Page 8.
"GHGs profiles have been rarely observed before near the experiment site, or over Northeast of China as far as we know. The model simulations are based on data of regional emission inventory. The accuracy of simulated profiles and concentration near surface over the experiment site still remains unknown. So continuous and regular observation of the GHGs profiles are necessary to better understand the regional emission amounts and the variation of the GHGs."

24. P7, L194: Did you use all these observations (aircore, balloon, aircraft) for your specific case or is this a general description? Is this Tan-Tracker? Please be more specific.

Response: The sentence "...high-altitude balloons, AirCore, Observations of the Middle Stratosphere balloon, and aircraft" refers to the data source used by TCCON's a prior profiles (Toon and Wunch, 2014). Due to altitude limit of flight, TCCON a prior profiles were used to extrapolate the profiles above the tropopause. As the other referee's comment mentioned, the use of any other profile will create additional biases when comparing to OCO-2 data, so we added another methods for extrapolation by using the a priori profile of OCO-2 as the supplement to the profile in the height where the measurement are not available.

Explanations as following are added in revised manuscript, Line 273, Page 9:
"Two extrapolation methods were used to extend the profile of the aircraft measurements and then estimates the X_{CO2} value of the in-situ measurement respectively. 1) The unknown part of the aircraft profile was directly from the OCO-2 a prior profile. 2) A well-mixed and constant mixing ratio of CO_2 is assumed from the surface to the lower limit of flight, and from the upper limit of flight to the tropopause. The CO_2 concentrations above the tropopause were calculated with an empirical model (Toon and Wunch, 2014) which considers tropopause height as well as realistic latitude and time dependencies through curve fitting of data from high-altitude balloons, AirCore, Observations of the Middle Stratosphere balloon, and aircraft. In general, the mole fraction of CO_2 decreased exponentially with height from the tropopause to upper stratosphere, and the tropopause height was obtained from NCEP reanalysis data with a 2.5° × 2.5° resolution, which was linearly interpolated to the geographic coordinates of Jiansanjiang. Figure 7 shows the extrapolated CO_2 profiles using method (2)"

25. P7, L197: This information come much too late (should be at the beginning of section 5.2).

Response: We moved this sentence to section 5.2, Page 8, Line 238.

26. P7, L199: You compare XCO2 values with the in-situ measured data. The variability of the latter is nearly 40 ppm, which is not at all captured by the OCO-2 average profile. In my opinion, you can´t compare column values and derive a bias (especially not with the accuracy given).

Response: Yes, you are right, the flight measurement were just obtained in limited altitude range, while the XCO2 is given for the whole atmosphere, therefore, they are not compared in the same level. But considering the low variation of CO2 with time in the high altitude of atmosphere, it is, at certain degree, reasonable to compare the XCO2 after the extension of the profile. To compare the uncertainty induced by the extension of the profile, results from two different extrapolation methods are used(table 4 in the revised manuscript). To assure the stable of the instrument, calibration and test against the standard gas is done just before the aircraft takeoff and checked again immediately after landing. figure 1 in the revised manuscript shows that the instrument is stable and accurate, almost no drift.

After considering the residence time of the airflow in the pipeline, and removing the data in 10-second average reprocess, the data shows much less variabilities.

27. Table 2: Please provide details on the uncertainty analysis for the aircraft errors: accuracy (traceability to WMO scale) and precision.

Response: As mentioned in previous response, calibration and test against the standard gas is done just before the aircraft takeoff and checked again immediately after landing, and the standard gas we used can be traced back to WMO scale. The average of the difference between the standard gas and the measurement of the instrument of each day was considered as the accuracy of the aircraft data. As for precision, the instrument was not continuously calibrated against the standard gas during the flight, 1-σ deviation of the measurements during level flight of each day is considered as the precision.

And we added sentences in the revised manuscript in Line 207, Page 7:

"The accuracy of CO2 and CH4 is below 0.66 ppm and 0.002 ppm, 0.16% and 0.10% of the CO2 and CH4 concentration in standard gas, respectively. For precision, the 1-σ value is below 0.71 ppm and 0.0062 ppm for CO2 and CH4, respectively"

The data of Table 2 (Table 4 in the revised manuscript) are corrected .

We added the following references to our manuscript:

Crisp, D., Miller, C., and DeCola, P.: NASA Orbiting Carbon Observatory; measuring the column averaged carbon dioxide mole fraction from space, J. Appl. Remote Sens., 2, 023508, doi:10.1117/1.2898457, 2008.

Endresen, Ø., Sørgård, E., Behrens, H. L., Brett, P. O. and Isaksen, I. S. A.: A historical reconstruction of

ships' fuel consumption and emissions, J. Geophys. Res. Atmos., 112(12), 1–17, doi:10.1029/2006JD007630, 2007.

Han, R. and Tian, X.: A dual-pass carbon cycle data assimilation system to estimate surface CO2 fluxes and 3D atmospheric CO2 concentrations from spaceborne measurements of atmospheric CO2, Geosci. Model Dev. Discuss., https://doi.org/10.5194/gmd-2019-54, in review, 2019.

Jung, Y., Kim, J., Kim, W. Boesch, H., Lee, H., Cho, C., and TaeYoung, G.: Impact of Aerosol Property on the Accuracy of a CO2 Retrieval Algorithm from Satellite Remote Sensing, Remote Sens., 8, 322, doi:10.3390/rs8040322, 2016.

Keller, C. A., Long, M. S., Yantosca, R. M., Da Silva, A. M., Pawson, S. and Jacob, D. J.: HEMCO v1.0: A versatile, ESMF-compliant component for calculating emissions in atmospheric models, Geosci. Model Dev., 7(4), 1409–1417, doi:10.5194/gmd-7-1409-2014, 2014.

Oda, T. and Maksyutov, S.: A very high-resolution (1km×1 km) global fossil fuel CO2 emission inventory derived using a point source database and satellite observations of nighttime lights, Atmos. Chem. Phys., 11(2), 543–556, doi:10.5194/acp-11-543-2011, 2011.

O'Dell, C. W., Connor, B., Bösch, H., O'Brien, D., Frankenberg, C., Castano, R., Christi, M., Eldering, D., Fisher, B., Gunson, M., McDuffie, J., Miller, C. E., Natraj, V., Oyafuso, F., Polonsky, I., Smyth, M., Taylor, T., Toon, G. C., Wennberg, P. O., and Wunch, D.: The ACOS CO2 retrieval algorithm – Part 1: Description and validation against synthetic observations, Atmos. Meas. Tech., 5, 99–121, doi:10.5194/amt-5-99-2012, 2012.

O'Shea, S. J., Bauguitte, S. J.-B., Gallagher, M. W., Lowry, D., and Percival, C. J.: Development of a cavity-enhanced absorption spectrometer for airborne measurements of CH4 and CO2, Atmos. Meas. Tech., 6, 1095–1109, https://doi.org/10.5194/amt-6-1095-2013, 2013.

Palmer, P. I., Parrington, M., Lee, J. D., Lewis, A. C., Rickard, A. R., Bernath, P. F., Duck, T. J., Waugh, D. L., Tarasick, D.W., Andrews, S., Aruffo, E., Bailey, L. J., Barrett, E., Bauguitte, S. J.B., Curry, K. R., Di Carlo, P., Chisholm, L., Dan, L., Forster, G., Franklin, J. E., Gibson, M. D., Griffin, D., Helmig, D., Hopkins, J. R., Hopper, J. T., Jenkin, M. E., Kindred, D., Kliever, J., Le Breton, M., Matthiesen, S., Maurice, M., Moller, S., Moore, D. P., Oram, D. E., O'Shea, S. J., Christopher Owen, R., Pagniello, C. M. L. S., Pawson, S., Percival, C. J., Pierce, J. R., Punjabi, S., Purvis, R. M., Remedios, J. J., Rotermund, K. M., Sakamoto, K. M., da Silva, A. M., Strawbridge, K. B., Strong, K., Taylor, J., Trigwell, R., Tereszchuk, K. A., Walker, K. A., Weaver, D., Whaley, C., and Young, J. C.: Quantifying the impact ofBOReal forest fires on Tropospheric oxidants over the Atlantic using Aircraft and Satellites (BORTAS) experiment: design, execution and science overview, Atmos. Chem. Phys.

Discuss., 13, 4127–4181, doi:10.5194/acpd-13-4127-2013, 2013.

Peters, W., Jacobson, A. R., Sweeney, C., Andrews, A. E., Conway, T. J., Masarie, K., Miller, J. B., Bruhwiler, L. M. P., Pétron, G., Hirsch, A. I., Worthy, D. E. J., van der Werf, G. R., Randerson, J. T., Wennberg, P. O., Krol, M. C. and Tans, P. P.: An atmospheric perspective on North American carbon dioxide exchange: CarbonTracker., Proc. Natl. Acad. Sci. U. S. A., 104(48), 18925–18930, doi:10.1073/pnas.0708986104, 2007.

Randerson, J. T., Werf, G. R. van der, Giglio, L., Collatz, G. J. and Kasibhatla, P. S.: Global Fire Emissions Database, Version 4, (GFEDv4).ORNL DAAC, Oak Ridge, Tennessee, USA. https://doi.org/10.3334/ORNLDAAC/1293., 2018.

Takahashi, T., Sutherland, S. C., Wanninkhof, R., Sweeney, C., Feely, R. A., Chipman, D. W., Hales, B., Friederich, G., Chavez, F., Sabine, C., Watson, A., Bakker, D. C. E., Schuster, U., Metzl, N., Yoshikawa-Inoue, H., Ishii, M., Midorikawa, T., Nojiri, Y., Körtzinger, A., Steinhoff, T., Hoppema, M., Olafsson, J., Arnarson, T. S., Tilbrook, B., Johannessen, T., Olsen, A., Bellerby, R., Wong, C. S., Delille, B., Bates, N. R. and de Baar, H. J. W.: Climatological mean and decadal change in surface ocean pCO2, and net sea-air CO2 flux over the global oceans, Deep. Res. Part II Top. Stud. Oceanogr., 56(8–10), 554–577, doi:10.1016/j.dsr2.2008.12.009, 2009.

Yevich, Rosemarie, and Jennifer A. Logan.: An assessment of biofuel use and burning of agricultural waste in the developing world, Global biogeochemical cycles, 17(4), doi: https://doi.org/10.1029/2002GB001952, 2003.

Response to Comments of reviewer2

The authors thank all reviewers for their constructive comments and suggestions, which have helped us to improve the quality of this paper both in sciences and writing. All comments are carefully considered and responded.

The manuscript by X. Sun et al. describes aircraft in-situ observations of CO2 and CH4 taken over Jiansanjiang, Northeastern China, between August 7 and 10, 2018. The authors used a turboprop aircraft which was limited to 0.6-7 km flight altitude. Therefore, the profiles only covered the upper part of the planetary boundary layer (PBL) and only part of the free troposphere. In general, I greatly appreciate the efforts of taking aircraft in situ observations of CO2 and CH4 and I understand their usefulness and limitations well. However, I think the focus of the manuscript is not balanced. Due to the limited altitude

coverage, the results would be most useful for validating the performance of Tan-Tracker, Carbontracker, CAMS or any other profile-based greenhouse gas data set. However, this is done only very briefly for Tan-Tracker and without much discussion about the obvious shortcomings of the model in the specific situation (active vegetation uptake of CO2 and CH4 emissions from rice fields) - especially near the surface. Instead, they spend most of the analysis and discussion on the comparison with the column-averaged OCO-2 XCO2 product - even though they correctly state that the largest error in this comparison comes from the unmeasured (extrapolated) part of their profiles.

My suggestion would be to rewrite sections 5.2 and 5.3 and put more emphasis on the profile comparison. This should include a more detailed analysis how biases near the surface influence the column-averaged XCO2 and XCH4 values.

Major issues: - concerning the profile to column comparison, the authors should also have a look at 1) J. Messerschmidt et al.: Calibration of TCCON column-averaged CO2 : the first aircraft campaign over European TCCON sites. Atmos. Chem. Phys., 11(21):10765– 10777, 2011. doi:10.5194/acp-11-10765-2011. 2) M. C. Geibel et al.: Calibration of column-averaged CH4 over European TCCON FTS sites with airborne in-situ measurements. Atmos. Chem. Phys., 12(18):8763– 8775, 2012. doi:10.5194/acp-12-8763-2012. Especially Geibel et al. discuss the effect of limited flight altitude on the column uncertainty due to extrapolation of the observed profiles in more detail than Wunch et al., 2010. - in Section 5.3, the authors should use the OCO-2 prior profile for extrapolating to the bottom and top of the atmosphere. The use of any other profile will create additional biases when comparing to OCO-2 data.

Thank you very much for the suggestions. We added analysis on the section 5.2 for profile comparison in our revised manuscript, Line 254, Page 9:

Response: *"GHGs profiles have been rarely observed before near the experiment site, or over Northeast of China as far as we know. The model simulations are based on data of regional emission inventory. So the accuracy of simulated profiles and concentration near surface over the experiment site still remains unknown. The continuous and regular observation of the GHGs profiles are necessary to better understand the regional emission amounts and the variation of the GHGs."*

We refer to the articles mentioned above, and revised extrapolation method of CO2 profile in the revised manuscript. One more method is used and estimated, in the additional method, CO2 concentration at altitude with no data is replaced by OCO-2 a priori profile directly.

We corrected the sentences in section 5.3 in the revised manuscript, Line 273, Page 9:

"Two extrapolation methods were used to extend the profile of the aircraft measurements and then estimates the XCO2 value of the in-situ measurement respectively. 1) The unknown part of the aircraft profile was directly from the OCO-2 a prior profile. 2) A well-mixed and constant mixing ratio of CO2 is assumed from the surface to the lower limit of flight, and from the upper limit of flight to the tropopause. The CO2 concentrations above the tropopause were calculated with an empirical model (Toon and Wunch, 2014) which considers tropopause height as well as realistic latitude and time dependencies through curve fitting of data from high-altitude balloons, AirCore, Observations of the Middle Stratosphere balloon, and aircraft. In general, the mole fraction of CO2 decreased exponentially with height from the tropopause to upper stratosphere, and the tropopause height was obtained from NCEP reanalysis data with a 2.5° × 2.5° resolution, which was linearly interpolated to the geographic coordinates of Jiansanjiang. Figure 7 (in the revised manuscript) shows the extrapolated CO2 profiles using method (2)."

And we added sentence in our revised manuscript, Line 297, Page 10:

"For method (1), since the value of CO2 mole faction of unknown part is the same as that of OCO-2 a-priori profile, as eq. (5) shows, no extra uncertainty would be introduced by extrapolation."

And the following sentences were added in our revised manuscript, Line 306, Page 10:

"Because of the lack of observation data near the surface, the missing measurement data was directly replaced by the data at the lowest altitude measured by the aircraft. The error caused by this practice is shown in table 3, with an average of 0.79 ppm for XCO2.This is also the impact of the lack of near-surface observations on the overall XCO2 estimates. Therefore, observations from near the surface to about 1 km from other method, such as in-situ GHG measurement by tethered balloon and high tower, is necessary for accurate estimation of XCO2."

Minor issues:

1. p. 2, l. 41-42: it is not true that passive satellite observations of GHGs can provide all-weather, all-day global coverage.

We corrected the sentences in our revised manuscript, Line 42, Page 2:

"... ,which can provide global coverage of the column-averaged dry-air mole fraction of CO_2 (XCO_2)."

2. p. 2, l. 51: the quantity X_gas as provided by TCCON as well as the satellite instruments is column-averaged dry-air mole fraction, not volume mixing ratio. Please check the definition of mole fraction vs. volume mixing ratio and replace "volume mixing ratio" throughout the text.

Thanks, We have checked the article and replaced the "mole fraction" and "volume mixing ration" to "column-averaged dry-air mole fraction" or "X_gas".

3. p. 3, l. 75: if possible, please provide references for all 3 satellites mentioned here.

The references are added in the article.

The following 4 references for, respectively, TanSAT, GMI/GF5 and GAS/FY3D are added in the article.

We corrected the sentences in our manuscript, Line 76, Page 3:

"Three satellites designed for CO2 measurement, TanSAT (Yang et al., 2018; Yang et al., 2020), GMI/GF-5 (Li et al., 2016), and GAS/FY-3D (Qi et al., 2020),…".

4. p. 4, l. 100: can these standard gases be referenced to the WMO GHG scale? And could you tell the nominal concentrations of CO2 and CH4 in these standards? Is isotopic composition of the standards an issue for the aircraft measurements?

Yes, the standard gases can be traced back to the WMO greenhouse GHG scale, which has been tested in some experiments. The concentration of the CO2 is 400.13 ppm and CH4 is 1.867 ppm of the standard. The standard gas we use has been measured in the laboratory for the proportion of δ13C in CO2. The range of the proportion is -8.0‰ to -8.2‰ close to the natural content, so it will not cause significant isotopic effect on the measurement of CO2 by optical method and meet the requirements of standard gas (Yao et al., 2013).

We added the details of the standard gas in our manuscript, Line 123, Page 4:

"The standard gas we used is…."

5. p. 4, l. 105: should be: "Aircraft measurements were carried out …"

We corrected this sentences in the revised manuscript as, Line 149, Page 5:

"Aircraft measurement were carried out from 7 to 10 August over Jiansanjiang (47.11°N, 132.66°E, 61 m above sea level), located in Heilongjiang province, Northeast China. Figure 2 shows the geolocation of the Jiansanjiang aircraft and the fight path."

6. p. 4, l. 109: are the mentioned times local or UTC? Please also provide the year for the dates!

Yes, the time mentioned here is local time, GMT+8.

We corrected the sentence in our revised manuscript, Line 154, Page 5, to "Three profiles were obtained between around 08:00 and 11:00 in local time (GMT+8) on 7, 9, and 10 August, 2018."

7. p. 4, l. 118: be consistent in the use of mixing ratio vs. mole fraction.

We replaced all the words "mixing ratio" to "mole fraction" to keep consistent.

8. p. 5, Eq. 3: all numbers should have units in this equation!

Thanks very much, we added the units to all the numbers in the Eq.3: $L_v = 2.500 \times 106\ J\ Kg{-1}$, M_w is the molecular weight of water equals to 18.016, $R = 8.3145\ J\ K{-1}mol{-1}$, and e_s (in hPa) at temperature T (in K).

We corrected the sentences in our revised manuscript, Line 184, Page 6:

"Where $L_v = 2.500 \times 106\ J\ Kg{-1}$, M_w is the molecular weight of water equals to 18.016, $R = 8.3145\ J\ K{-1}mol{-1}$, and e_s (in hPa) at temperature T (in K)."

9. p. 5, l. 138-151: can you derive the planetary boundary layer height from your meteorological data, e.g by calculating the Bulk-Richardson number or some other indicator?

Sorry, the meteorological obtained aircraft is limited and we did not have the actual wind speed value of the atmosphere required for calculation of the Bulk-Richardson number.

10. p. 6, l. 160: the use of the word "accurate" here is misleading. If Tan-Tracker has been validated for

accuracy, please provide a number. Or just drop "accurate". Besides, the aircraft observations show that the accuracy of Tan-Tracker here is limited.

Thank you, we remove the word "accurate" from the sentence.

11. p. 8, l. 219: why is one given in ppm and the other in percent?

Sorry for the sentence is misleading and the it is corrected as (Line 319, Page 11) "... , but the values of mole fraction of CO2 from Tan-Tracker and OCO-2 had negative bias estimates. The average bias between aircraft and OCO-2 is −4.68 ± 2.02 ppm (1.18 ± 0.11%)."

12. p. 8, data availability: it would be nice if at least the 3 profiles were provided as a supplement to the paper. The amount of data should be rather small.

Yes, all the 3 profiles and relative meteorological data such as profiles of temeratureare, pressure and w ater vapor are available from corresponding author upon request (dmz@mail.iap.ac.cn) .

13. C3- Fig. 1: the black-and-white map of China is not very appealing. Also, a close-up of the target region, potentially as a terrain map or satellite picture would be illustrative.

Fig.1 (figure 2 in the revised manuscript)was replotted and added the flight path over the google map, we zoom in the figure focusing on the area near the experiment site.

14. - Figs. 3-5: an indication of PBL height would be useful on all these figures.

Because of the height limitation of the data, the PBL height cannot be calculated from it. So we used PBL height from reanalysis product ERA-Interim (https://www.ecmwf.int/en/forecasts/datasets/reanalysis-datasets/era-interim) with the spatial resolution of 0.125° × 0.125°, spatially and time averaged to the flight area and time. We revised the figure 5 (figure 8 in the revised manuscript).

15. - p. 15/16, Table 2: I assume that the numbers are for CO2 but it is not actually mentioned in the table captions. If so, a similar table for CH4 would be useful. I would also appreciate an estimate of the

total resulting uncertainty.

Since OCO-2 only provide CO2 products, we do not provide the table of uncertainty of estimate XCH4. But we can provide the precision and accuracy of the CH4 measurement of the aircraft. The maximum and the average value of the difference between the standard gas and the measurement of the instrument of each day was given, and represent the accuracy of the aircraft data. For the precision, we calculated the one standard deviation of the data in each level flight, and the average and maximum value of 1-σ on each day is considered as the precision of the aircraft measurement.

The numbers on table 2 are for CO2, and we added the it to the introduction of the table:
" Table 2. Aircraft integration error budget of XCO2 estimation…"

We added the following references to our manuscript:

Li Y. F., Zhang C. M., Liu D. D., Chen J., Rong P., Zhang X. Y., Wang S. P. CO2 retrieval model and analysis in short-wave infrared spectrum. Optik, 127, 4422-4425, doi:10.1016/j.ijleo.2016.01.144, 2016.

Qi C., Wu C., Hu X., Xu H., Xu H., Lee L., Zhou F., Gu M., Yang T., Shao C., Yang Z. High spectral infrared atmospheric sounder (HIRAS): system overview and on-orbit performance assessment. IEEE Trans. Geosci .Remote Sens., PP, 1-18, doi:10.1109/TGRS.2019.2963085, 2020.

Yao, B., Huang, J.Q., Zhou, L.X., Fang, S.X., Liu, L.X., Xia, L.J., Li, P.C., Wang, H.Y. Preparation of mixed standards for high accuracy CO2/CH4/CO measurements. Environ. Chem., 02:135-140, doi:10.7524/j.issn.0254-6108.2013.02. 019, 2013.

Yang Z., Zhen Y., Yin Z., Lin C., Bi Y., Wu Liu., Wang Q., Wang L., Gu S., Tian L. Prelaunch Radiometric Calibration of the TanSat Atmospheric Carbon Dioxide Grating Spectrometer. IEEE Trans. Geosci. Remote Sens., 56, 4225-4233, doi:10.1109/TGRS.2018.2829224, 2018.

Yang Z., Bi Y., Qian W., Liu C., Gu S., Zheng Y., Lin C., Yin Z., Tian L. Inflight Performance of the TanSat Atmospheric Carbon Dioxide Grating Spectrometer. IEEE Trans. Geosci .Remote Sens., PP, 1-13, doi:10.1109/TGRS.2020.2966113, 2020.